Articles in PresS. J Neurophysiol (March 24, 2010). doi:10.1152/jn.01008.2009

Cue reliability and a landmark stability heuristic determine relative weighting between egocentric and allocentric visual information in memory-guided reach.

Patrick A. Byrne[1,2] and J. Douglas Crawford[1, 2,,3]

[1]Centre for Vision Research, York University, Toronto, Canada

[2]Canadian Action and Perception Network

[3]Neuroscience Graduate Diploma Program and Departments of Psychology, Biology, and Kinesiology and Health Sciences, York University, Toronto, Canada

RUNNING HEAD: Landmark stability important for ego/allocentric weighting

Contact Info:
J. Douglas Crawford
Centre for Vision Research, York University
4700 Keele Street, Toronto, ON, Canada M3J 1P3
email: jdc@yorku.ca
Tel: (416)736-2100 x88621
Fax: (416)736-5857

ABSTRACT

It is not known how egocentric visual information (location of a target relative to the self) and allocentric visual information (location of a target relative to external landmarks) are integrated to form reach plans. Based on behavioural data from rodents and humans we hypothesized that the degree of stability in visual landmarks would influence the relative weighting. Furthermore, based on numerous cue-combination studies we hypothesized that the reach system would act like a maximum-likelihood estimator (MLE), where the reliability of both cues determines their relative weighting. To predict how these factors might interact we developed an MLE model that weighs egocentric and allocentric information based on their respective reliabilities, and also on an additional stability heuristic. We tested the predictions of this model in 10 human subjects by manipulating landmark stability and reliability (via variable amplitude vibration of the landmarks and variable amplitude gaze-shifts) in three reach-to-touch tasks: an egocentric control (reaching without landmarks), an allocentric control (reaching relative to landmarks), and a cue-conflict task (involving a subtle landmark 'shift' during the memory interval). Variability from all three experiments was used to derive parameters for the MLE model, which was then used to simulate egocentric-allocentric weighting in the cue-conflict experiment. As predicted by the model, landmark vibration –despite its lack of influence on pointing variability (and hence allocentric reliability) in the control experiment— had a strong influence on egocentric-allocentric weighting. A reduced model without the stability heuristic was unable to reproduce this effect. These results suggest heuristics for extrinsic cue stability are at least as important as reliability for determining cue weighting in memory-guided reaching.

Keywords: memory-guided reaching, visuomotor transformation, egocentric, allocentric, maximum-likelihood integration, human psychophysics

INTRODUCTION

Goal directed actions –such as a reaching toward a briefly viewed target— often depend on feed-forward movement plans, either because of the demands of movement speed (Carlton 1981; Keele and Posner 1968; 1991; Zelaznik et al. 1983), because visual gaze is needed for some other purpose (e.g. Flanagan et al. 2008), or because the target is no longer visible (Blohm and Crawford 2007). The latter is often simulated in laboratory conditions, but it also occurs in natural behaviors –such as hunting and gathering— where the object of interest frequently becomes obscured, for instance by a bush. In these situations the brain must construct internal spatial representations of target location and use these in a feed-forward fashion to guide the movement (Ariff et al. 2002; Flanagan et al. 2001; Flanagan et al. 2003; Robinson 1981).

In theory there are two general ways to encode and remember the locations of visual targets for action: relative to the self (egocentric coding) or relative to other external landmarks (allocentric coding). For example, imagine a prehistoric hunter chasing his prey through the savanna. Suddenly, his quarry disappears into tall grass. At this point the hunter has two ways to aim a spear throw toward the hidden quarry. First, he might rely on egocentric information: the (perhaps fading) memory of the last location at which the target was visible (i.e., where it stimulated his retinas, taking into account where his eyes were pointing at the time). Alternatively, he might rely on allocentric information: the memory of the animal's last visible location relative to some salient landmark (like a tuft of differently colored grass in his visual field).

In real-world circumstances, both types of cue, egocentric and allocentric, are normally available for the brain to use. Egocentric information is always present in healthy subjects, and many studies have shown that subjects can reach and point with reasonable accuracy to

77 remembered targets based solely on egocentric cues (Batista et al. 1999; Blohm and Crawford
78 2007; Buneo et al. 2002; Crawford et al. 2004). In most natural cases allocentric information can
79 also be derived from the environment, and it has been shown that this can have a strong influence
80 on remembered target location (Krigolson et al. 2007; Krigolson and Heath 2004; Obhi and
81 Goodale 2005). The question, then, is how are these cues combined and weighted by the brain?
82 Numerous studies have attempted to differentiate the factors that determine the relative
83 importance of these different cues. Diverse variables have been found to play an important role,
84 including age (Hanisch et al. 2001; Lemay et al. 2004), memory delay (e.g. Carrozzo et al. 2002;
85 Glover and Dixon 2004; Hay and Redon 2006; Obhi and Goodale 2005), context (Neely et al.
86 2008), and demand characteristics (Bridgeman et al. 1997). Allocentric information can also
87 affect reaching movements differentially depending on the relative alignment between effector
88 movement direction and intrinsic landmark geometry (de Grave et al. 2004). Furthermore, it has
89 been suggested by many that allocentric information tends to dominate over egocentric when the
90 former is present, at least when action occurs after a memory delay (e.g. Lemay et al. 2004;
91 Neggers et al. 2005; Sheth and Shimojo 2004). However, to our knowledge, the computational
92 rules used to weight between such cues have not been tested or modeled.
93 One factor that is likely to influence the weighting of egocentric and allocentric
94 information is the relative *reliability* of these two sources of information. In practice, the
95 reliability of cue is taken to be the inverse of the variance in repeated behavioral responses based
96 solely on that cue (for a recent experimental example, see Brouwer and Knill 2009). As a 'real
97 world' example, when our hunter bases his spear throws on distal landmarks, he might find that
98 he has more difficulty hitting his target (the endpoint of his spear toss might be more variable
99 over repeated throws) than if he relied on nearby landmarks. In the former case, when only distal

landmarks are available, he might tend to give more weight to his own egocentric memory of target location than he would in the latter case in order to compensate. From numerous experimental studies requiring subjects to respond based upon two or more estimates of a given stimulus dimension, it has been found that the relative influence of these multiple cues is, at least in part, determined by their respective reliabilities, as measured from response variability in single cue control tasks (e.g. Battaglia et al. 2003; Ernst and Banks 2002; Knill 2007b; Knill and Saunders 2003; van der Kamp et al. 1997; Vaziri et al. 2006). Thus, we expect any putative combination rule for egocentric and allocentric spatial cues to show similar dependence.

Although in many cases the brain does appear to combine multiple information sources based on *accurate* estimates of individual cue reliabilities, this need not always be the case. The brain might also derive heuristic rules for judging cue reliability through prior experience or evolutionary hardwiring. Returning again to our hunter story, if a strong wind was causing the landmark (the colored tuft of grass) to wave back and forth and change shape, the hunter's brain might discount this landmark as unreliable, even though its average position in fact remains rooted in the same location. This might be because in previous cases his visual system noticed that loose vegetation blowing in the wind has no value as an allocentric cue, and thus has learned to place less trust on anything in motion. We refer to such putative down-weighting of allocentric information as a 'stability heuristic', that, if it exists, likely results from expectations about the usefulness of landmarks. Presumably, spatial information derived from apparently stable landmarks would weigh more heavily in an egocentric-allocentric combination than would information derived from apparently unstable ones. This question has been addressed in several studies of spatial cognition (Biegler and Morris 1996a; Biegler and Morris 1993, 1996b; Burgess et al. 2004; Jeffery 1998). For example, place-cells in the rat may cease to fire for landmarks that

123 are shifted in the presence of the animal (Jeffery 1998). Likewise, rats will only learn the
124 locations of food rewards relative to landmarks if those landmarks are stable Biegler and Morris
125 (1996a, 1993, 1996b). Similarly, humans perform better in spatial memory tasks when visual
126 landmarks never change location in the presence of the subject (Burgess et al. 2004). However,
127 to our knowledge, the behavioural consequences of variable apparent landmark stability on cue-
128 combination have not been investigated directly and quantitatively in any studies of human
129 visuomotor control.

130 In order to simultaneously test the influence of these factors (actual egocentric and
131 allocentric reliabilities, and heuristically-based judgements of landmark reliability) it is
132 necessary to make quantitative predictions. This is not trivial. For example, introducing
133 instability in landmarks might affect both the actual reliability of allocentric information (as
134 judged from response variability in a task where only allocentric information can be used) *and*
135 activate the putative stability heuristic. These factors, along with estimates of egocentric
136 reliability might then interact in very complex ways, especially when one is dealing with a two-
137 dimensional array of targets. Previous studies of both perception and action have dealt with such
138 problems by using a maximum-likelihood estimator (MLE) (e.g. Battaglia et al. 2003; Ernst and
139 Banks 2002); (Knill 2007b; Knill and Saunders 2003; van der Kamp et al. 1997; Vaziri et al.
140 2006). An MLE model allows one to predict how multiple stimulus estimates with different
141 reliabilities should combine in a statistically optimal fashion, which is exactly what we needed to
142 do here.

143 In the current study we directly tested the hypotheses that 1) reaching to remembered
144 targets is guided by an internal weighting process that combines egocentric and allocentric
145 information, 2) that allocentric information derived from apparently unstable landmarks is

weighed less than that derived from apparently stable ones (because of a stability heuristic), and that 3) this weighting process is also reliability-dependent. We did this by first developing an MLE model of reaching that relied on both cue reliability and the stability heuristic. Within the model, the stability heuristic was represented via a 'stability parameter' that affected weighting of egocentric and allocentric information by modulating the influence of the actual reliability of the latter. Second, we experimentally derived the parameters of this model. Finally, we used the fitted model to simulate and predict the results of a reach-to-touch paradigm in which a spatial conflict between egocentrically and allocentrically defined target locations was induced, and in which the stability of visual landmarks and the actual reliability of egocentric information were systematically varied. As predicted by our model and confirmed in the results, both the stability heuristic and the actual reliability of egocentric and allocentric information contributed to the relative weighting of these cues.

METHODS

Theory and Design

An MLE rule weighs multiple estimates in proportion to their reliabilities. Such rules have been found to act across modalities (e.g. Battaglia et al. 2003; Ernst and Banks 2002) and within the visual modality alone (Knill 2007b; Knill and Saunders 2003; van der Kamp et al. 1997; Vaziri et al. 2006). If landmark stability influences egocentric-allocentric weighting, it might do so in at least two ways. First, as suggested by the experiments of Burgess et al. (2004) (and others described above), there might be some internal stability heuristic that causes the brain to down-weigh the contribution of allocentric information based on landmarks that do not appear to be fixed at a particular location. This effect would be independent of the actual

reliability of the allocentric information. Second, it might be more difficult to localize a target relative to landmarks that undergo any kind of movement, even if the movement could, in principle, be averaged out. Down-weighting of allocentric information in this latter case would be reliability-dependent.

Since we framed our hypotheses in terms of an MLE model, it was necessary to develop this model in concert with the experimental design such that 1) some aspects of the data could be used to fit the model parameters, whereas 2) other aspects of the data could be used to test the model (importantly, while maintaining mutual independence between these two procedures). In brief, there were three tasks in which subjects reached to touch the remembered location of a visual target flashed briefly on a computer screen in complete darkness, after a memory delay. These tasks consisted of a *cue-conflict* experiment (Figure 1A) in which egocentric and allocentric cues conflicted at test because of a subtle landmark shift during the memory delay, and two controls: an *egocentric-variability* control (Figure 1B) designed to measure reaching variability when no landmarks were present, and an *allocentric-variability* control (Figure 1C) designed to measure reaching variability when reaching could depend *only* on visual landmarks. Visual landmarks were chosen to be similar to those of Krigolson and Heath (2004), which have been shown to generate significant improvement in reaching accuracy to remembered targets.

To this basic design we added the following manipulations. First, we manipulated stability of landmarks (in both the cue-conflict experiment and the allocentric control) by imparting a vibration to them. The main intent of this manipulation was to confirm the existence of the stability heuristic in egocentric-allocentric weighting, but it was also possible that this manipulation would affect the actual reliability of allocentric information. Our allocentric control experiment allowed us to measure the latter via response variability and incorporate this into the

MLE model. Second, we added another manipulation to produce corresponding variations in the reliability of the egocentric channel. It has been shown that efference copies of eye position and eye movement are used to update and maintain spatial representations within the brain (e.g. Niemeier et al. 2003), and that increasing the amplitude of gaze shifts that occur during a memory interval increases the amount of noise in spatial memory (Prime et al. 2006; Prime et al. 2007). Thus, during the memory delay we manipulated egocentric reliability by varying total gaze movement amplitude during the memory interval. Our egocentric control allowed us to independently measure the effects of this manipulation and incorporate this into our model.

We modeled the stability heuristic by adding a 'stability parameter' to our MLE model (see below for model details) that artificially deflates the reliability estimate for allocentric information when landmarks are unstable. This introduced the problem of how to determine a value for this parameter. Normally, testing an MLE model of cue-combination involves measuring cue reliability from response variability in single-cue control tasks. From these reliability estimates, the MLE model can be used to predict how subjects will weigh the various cues when these are simultaneously present, but possibly in conflict (e.g. Smeets et al. 2006; van Beers et al. 1999). In order to obtain estimates for egocentric and allocentric reliability, of motor noise, and an estimate for the stability parameter, we instead followed procedures similar to those of Brouwer and Knill (2009). These authors noted that MLE models predict a specific relationship between response variability in single-cue control tasks and variability in a corresponding multi-cue task. In our case the stability parameter also entered into this relationship. Therefore, we could use this relationship between reaching *variability* in all three of our tasks to obtain estimates of egocentric and allocentric reliability, of motor noise, and of the stability parameter. These estimates were then incorporated into our MLE model and used to

predict what the *weighting* should be between egocentric and allocentric cues in our cue-conflict experiment (see Figure 2 for a graphical illustration of our procedure). Note that our procedure for determining the value of our stability parameter is not novel; for example, McGuire and Sabes (2009) used a similar approach to determine values for non-reliability related parameters in their MLE model.

The mathematical details of our MLE model are presented below (and in the Appendix) after a description of the experimental procedures used to obtain the reaching dataset.

Participants

A total of ten right-handed human subjects participated in all three experiments; six females and four males between the ages of 20 and 49. Nine of the ten subjects were naïve to the design and purpose of the experiment, while one was naïve only to the design. This latter subject showed results that did not differ qualitatively from the remaining subjects. All subjects had normal or corrected to normal vision and none of these subjects had any known neuromuscular deficits. All subjects gave informed consent and all procedures involved in the experiment were approved by the York Human Participants Review Subcommittee.

Apparatus and Stimuli

Subjects were seated in total darkness with the head fixed using a bite bar apparatus with a personalized dental impression. The heights of the seat and bite bar were adjusted independently so that the nasal root was vertically and horizontally aligned with the centre of a CRT display (Dell). The screen had vertical and horizontal screen dimensions of 30 cm (1024 pixels) and 40.5 cm (1280 pixels), a refresh rate of 70 Hz, and was situated 40 cm directly in front of the subject. In order to eliminate background luminance (stimuli were presented on a black background in a

completely dark room) the CRT brightness was set to the minimum setting and a light absorbing film was applied to the screen surface. All stimuli were displayed on this screen, with the exception of a beep that indicated when subjects were to reach. Two 40 Watt desk lamps, one placed on either side of the CRT display, were also turned on automatically at regular intervals (see below) in order to eliminate dark adaptation. Between trials the subject was instructed to return their fingertip to a home location positioned near the bottom right corner of the CRT on the table that supported it. At this location a coin was glued to the table to provide a distinctive surface. With their fingertip at the home location the subject's arm was resting comfortably on a table at the same height as the base of the CRT display.

Reaching responses were measured using a two camera Optotrak 3020 (Northern Digital) tracking system. These cameras continuously recorded (sampling frequency of 150 Hz) the 3-D positions of three infrared-emitting diodes (IREDs) placed along the right index finger, with one near the fingertip, another approximately 1 cm more proximal along the finger, and another approximately 1 cm further proximal. IRED position data from the Optotrak was not filtered. Gaze-direction was continuously monitored (sampling frequency of 120 Hz) by a head-mounted infrared eye-tracking system (Applied Science Laboratories) that monitored the left eye. Eye-tracking data was filtered to remove rapid signal changes corresponding to unnatural eye movement speeds of greater than 1000 deg/s. This was accomplished simply by removing the data starting at the high speed movement onset and the point of return to pre-movement baseline. The empty space was interpolated if it did not last more than 400 ms, otherwise the trial was discarded. The same interpolation procedure was used to remove eyeblinks.

All stimuli were generated with a Windows-based Pentium 4 PC (Dell) using MATLAB 6.5 (The MathWorks) along with the Psychophysical ToolBox v3.0.8 (Brainard 1997; Pelli

1997). The to-be-remembered target stimulus consisted of a single, filled yellow disc with a diameter of one degree visual angle. For a given trial, this target stimulus could appear anywhere on a circular annulus with inner radius of 11 degrees and outer radius of 13 degrees centered at the screen center. The visual landmarks consisted of four identical blue discs, each with a diameter of one degree, positioned at the vertices of a virtual square with a seven degree edge length. On any given trial this virtual square was positioned so that the to-be-remembered target occupied a random location within a smaller central square region of 60% of the width of the full virtual square. Furthermore, the virtual square, and hence the collection of visual landmarks, would vibrate about its average position with either a small or large amplitude. In particular, the small vibration amplitude was chosen so that each individual landmark in this condition maintained a relatively large region of overlap with its initial position at all times. Thus, landmarks in this condition were taken as 'stable' because they appeared to wobble about in place but not to change location completely. We chose the large vibration amplitude such that each individual landmark maintained no constant region of overlap with itself and thus appeared to move from place to place within a limited region of space. In both low vibration amplitude (stable) and high vibration amplitude (unstable) conditions the landmarks had well-defined average locations (i.e. there was no net 'drift') and could, in principle, have been equally useful to subjects. Our assumption here was that the relatively unstable, larger vibration amplitude landmarks would be judged as less useful by subjects as an allocentric cue. The vibration itself consisted of independent horizontal and vertical sinusoidal motion, with horizontal and vertical oscillation frequencies on each trial being chosen randomly and independently from the range [6.67,10] Hz. Choosing both vibration frequency components independently ensured that the overall motion did not appear to be circular. The small and large vibration amplitudes were

chosen to be 0.2 and 0.6 degrees, respectively, which satisfied the definitions of stable and unstable given above.

Visual fixation during the experiment was controlled by means of a fixation cross consisting of two identical bars that had a width of 0.17 degrees and a length of 0.67 degrees. At the beginning of each trial and throughout target presentation the fixation cross would be present at the center of the screen. Gaze shifts of either small or large amplitude were generated by having the fixation cross make a sequence of two jumps. During such a sequence, the cross would first disappear from the screen center and then reappear at an intermediate location 100 ms later. After 750 ms the cross would disappear again and reappear at its final location 100 ms later. The intermediate and final locations were chosen randomly within two constraints: 1) the final location had to be within a disc of six degrees radius centered at the original location, and 2) the overall movement amplitude had to be either small (10 degrees) or large (30 degrees). Throughout this sequence subjects were required to follow the cross with their eyes.

Experimental paradigm

The entire experiment consisted of three sessions, the first of which was the main cue-conflict experiment, the second session was the egocentric-variability control experiment, while the third was the allocentric-variability control experiment. All sessions were performed on separate days separated by two weeks or more. Each session also began with a simple calibration block that allowed IRED positions to be converted easily into screen-relative reach endpoint coordinates. The two control experiments were run after the cue-conflict experiment in order to ensure that they did not somehow affect the behaviour of subjects in the main experiment.

Cue-conflict experiment

Each trial of the cue-conflict experiment (see Figure 1A) began with the subject fixating the centrally-presented cross for 2 s. At the end of this period the yellow target disc and vibrating visual landmarks would appear for 1.5 s, with the target situated randomly within the centered annulus and the landmarks situated relative to the target as described above. Although the visual landmarks would vibrate whenever present, the target itself was always perfectly stationary whenever visible. Trials with small or large vibration amplitude, i.e. stable or unstable trials, were randomly interleaved. Furthermore, subjects were explicitly instructed to *ignore* the "vibrating blue dots". Following a 500 ms delay after target/landmark offset the fixation cross would execute the small or large movement sequence described above, with small and large movement trials randomly interleaved. In total then, we had four unique experimental conditions, v. These were *sv_sgs (small landmark vibration-small gaze shift), sv_lgs (small landmark vibration-large gaze shift), lv_sgs (large landmark vibration-small gaze shift),* or *lv_lgs (large landmark vibration-large gaze shift).* In order to introduce cue-conflict the vibrating landmarks would reappear 300 ms after completion of the eye-movement sequence for another 1.5 s, but with their collective center shifted in a random direction by three visual degrees. The rationale here was that the shift in landmarks should have had no effect on an egocentric memory of target location, but that reaching based upon allocentric information would be shifted with the landmarks. Thus, the location that the target would occupy if it had shifted with the visual landmarks will be referred to from here on as the *allocentric location.* At landmark offset the fixation cross would disappear and the subject would hear a beep indicating that they should touch the screen at the remembered location of the yellow target disc. Subjects were allowed to direct their gaze freely throughout the reaching phase. After another 2.5 s a second, return-signal

beep would sound indicating that the subject should return their finger to the home position. The next trial would begin immediately. Every fifth trial was a "throwaway" trial during which the 40 Watt lamps were illuminated to prevent dark adaptation. After every 20 trials subjects were given a 35 s rest period during which the lamps were illuminated. In total subjects performed 130 non-illuminated trials, with results from the first ten discarded as practice trials. Sample eye and finger traces for one subject are shown in Supplementary Figure S1.

Egocentric-variability control experiment

The egocentric-variability control experiment is depicted in Figure 1B. The procedure for this control experiment was identical in all aspects to the main experiment described above, with the exception that no landmarks were ever presented. Thus, subjects presumably only ever had egocentric information about target location to work with. Again, every fifth trial was a "throwaway" trial during which the 40 Watt lamps were illuminated to prevent dark adaptation. After every 20 trials subjects were given a 35 s rest period during which the lamps were illuminated. In total subjects performed 90 non-illuminated trials, with results from the first ten discarded as practice trials.

Allocentric-variability control experiment

The allocentric-variability control experiment is shown in Figure 1C was nearly identical to the main experiment. There were three differences. First, subjects were instructed explicitly to remember where the target was *relative* to the "vibrating blue dots". Second, the small shift in location of the vibrating visual landmarks from first to second presentation was accompanied by an additional, large translational shift. In order to generate this shift, the vector connecting the subject's nasal root and the original landmark centre of geometry was rotated about the axis

connecting the subject's nasal root and the screen centre by a random angle of between 45 and 315 degrees. The tip of this rotated vector was taken as the new centre of geometry for the *translated* landmarks. Thus, the location of the landmarks on their second presentation was unrelated to their location during the first presentation, but was subject to the same overall constraints on possible location. Third, during the reaching phase of this task, subjects were required to touch to the location that the target would have had if it had shifted with the landmarks.

Optotrak calibration

This calibration session consisted of 20 simple trials in which the head-fixed subject would reach to touch a yellow target disc that would appear at a random location within the centered annulus described above. IRED position data in the Optotrak intrinsic coordinate system was then combined offline with the known screen coordinates for the various target presentations to generate a linear mapping between IRED position and screen coordinates. This procedure eliminated the need to place precisely the CRT screen relative to the Optotrak coordinate system, and it eliminated the need to place precisely and identically the IREDs on the fingers of different subjects.

Data Analysis

All data analysis occurred offline using custom software written in MATLAB (The MathWorks). Each trial from all experimental sessions (calibration, egocentric-variability control, allocentric-variability control, and main cue-conflict experiment) involved a reaching response phase that began with a beep signaling the start of reaching, a 2.5 s movement period, and a second, return-signal beep indicating that the subject was to return their finger to the home location. Any trial in

which the subject's finger moved faster than 1 cm/s before the start signal was discarded. In order to determine IRED coordinates for a given reaching response the Optotrak-measured IRED positions were averaged over an approximately 300 ms period that occurred within the movement period and in close temporal proximity to the corresponding return-signal beep. For most trials this averaging period began 300 ms before the return signal and ended at the return signal. However, sometimes a subject would begin returning their fingertip early or would make a finger movement exceeding a criterion velocity of five cm/s within this time period. In such cases the last 300 ms period preceding the return signal in which the velocity criterion was not exceeded was selected as the averaging period. This was done, as opposed to choosing one decelaration point (as just one on many examples, see Krigolson et al. 2007), in order to ensure subjects had reached their final selected position and to smooth out irrelevant noise (e.g. van Beers et al. 1999).

In order to generate a mapping between IRED coordinates and screen-relative coordinates of the fingertip at the end of a reaching movement the known screen coordinates of the target presentations in the calibration sessions were regressed against IRED coordinates determined using the averaging procedure described above. This regression was a simple least-squares fitting of an eight parameter linear model. Once the calibration parameters were determined IRED coordinates of a reaching endpoint could be mapped to screen-relative coordinates for the control and main experiment sessions. The fitting procedure was carried out independently for each of the three IREDs, and the IRED that generated the fit with the smallest Predicted Residual Sum of Squares (Allen 1974) statistic was used to determine screen-relative reaching endpoints in the subsequent control or main experiment session. This measure is more

appropriate than a simple R^2 value because it measures the predictive ability of the fit – exactly what we wish to know.

During each trial of the control or main experiments fixation was deemed acceptable if gaze did not deviate from the cross by more than +/-1 degree in the horizontal or vertical direction. The gaze shift sequence was deemed acceptable if: 1) the first eye movement began after the cross appeared at the intermediate location and reached the cross at this location before it disappeared, and 2) the second eye movement began after the cross appeared at its final location and reached the cross at this location within 300 ms of its appearance (thus ensuring gaze was properly located at the start of the second landmark presentation phase). Any trial in which gaze shifts did not satisfy these criteria was discarded. Furthermore, the raw data was trimmed of outliers using the Chauvenet procedure (Taylor 1997). For both control experiments the correct target location for a given trial was subtracted from the raw reaching endpoint to generate a set of target-relative responses. The Chauvenet procedure was applied to both the x and y components of the set of target-relative reaching endpoints for each subject/condition conjunction. In the main cue-conflict experiment the model in Equation 1 was fit to the raw data for each subject/condition conjunction and the Chauvenet procedure was applied to the x and y components of the fit residuals.

In the main cue-conflict experiment target location, landmark shift direction, and landmark position relative to target were chosen random within the previously described constraints. In order to make data from each trial comparable the transformation process depicted in Figure 3A was performed on the reaching data. First, reaching endpoints for a given subject were corrected to remove any systematic reaching bias (not depicted in the Figure). That is, the vector connecting target and reaching endpoint for a given trial was averaged across all

conditions and trials for a given subject and was subtracted from all of that subject's individual reaching endpoints. Next, the corrected reaching endpoint from a given trial was transformed by the unique set of translation, rotation, and scaling operations that would bring the original target location and allocentric location, if similarly transformed, to the origin and the (1,0) position of the new coordinate system, respectively. The x-component of this transformed reaching endpoint will be referred to as its *allocentric weight*. Thus, an allocentric weight of 0 would imply a reaching endpoint at the original target location (neglecting the component perpendicular to the shift direction) and an allocentric weight of 1 would imply a reaching endpoint at the allocentric location (the location of the target if it had shifted with the landmarks). Note: when we fit our MLE model below, we fit it to the raw data without any of the above transformations.

For the control experiments a measure of overall variable reaching error relative to target location was required for each combination of subject and eye-movement/vibration amplitude condition (small/large). Each reaching endpoint (in screen coordinates) for a given combination was translated by subtracting from it the actual target location on that trial. The *overall reaching variance* estimate of these target-relative responses was taken to be the root-mean-square of the eigenvalues of their covariance matrix. We chose this measure because it behaves like the area of a confidence ellipse for relatively isotropic reaching endpoint distributions, but more like a one-dimensional variance for highly elongated distributions. In the latter case one could in principle find a confidence ellipse that was very long in one dimension, but short enough in the other that it maintained a relatively small area. In this case area would not be a particularly good measure of reaching variability.

Details of Model.

When reaching for a target we assumed that the brain relies on at least two estimates of target location, $\hat{\mathbf{r}}_{\mathrm{a};\nu,s}$ and $\hat{\mathbf{r}}_{\mathrm{e};\nu,s}$, where $\hat{\mathbf{r}}_{\mathrm{a};\nu,s}$ is an allocentric estimate based on visual landmarks and $\hat{\mathbf{r}}_{\mathrm{e};\nu,s}$ is an egocentric estimate. Here, ν refers to the collection of conditions under which the target is perceived and the reaching takes place, while *s* refers to the fact that these estimates might vary systematically between individual subjects, even under otherwise identical conditions. We further assumed that these estimates are bivariate normal random variables (we restrict the model to two spatial dimensions here) with expectation values of $\mathbf{r}_{\mathrm{a}}$ and $\mathbf{r}_{\mathrm{e}}$, the actual allocentrically and egocentrically-defined target locations, and covariances of $\boldsymbol{\Sigma}_{\mathrm{a};\nu,s}$ and $\boldsymbol{\Sigma}_{\mathrm{e};\nu,s}$. The overall form of our model was chosen to be a simple, but general linear mapping of the form

$$\mathbf{r}_{\mathrm{p}} = \mathbf{M}_{\nu,s}\left\{\mathbf{W}_{\nu,s}\hat{\mathbf{r}}_{\mathrm{e}_{\nu,s}} + \left(\mathbf{I} - \mathbf{W}_{\nu,s}\right)\hat{\mathbf{r}}_{\mathrm{a}_{\nu,s}}\right\} + \mathbf{b}_{\nu,s} + \boldsymbol{\epsilon}_{s}^{\mathrm{m}}\ , \qquad (1)$$

where $\mathbf{r}_{\mathrm{p}}$ is the subject's reaching endpoint, $\mathbf{W}_{\nu,s}$ is a two dimensional weight matrix, and $\boldsymbol{\epsilon}_{s}^{\mathrm{m}}$ is additive bivariate normal motor noise. Here we have assumed that the egocentric-allocentric integrator is unbiased, but that the result may be affected by small, systematic distortions, which we modeled linearly via the multiplicative matrix, $\mathbf{M}_{\nu,s}$, and the constant offset vector, $\mathbf{b}_{\nu,s}$. A similar modeling scheme has been used successfully elsewhere (Brouwer and Knill 2009) for a one-dimensional task. For simplicity, we can rewrite Equation 1 as

$$\mathbf{r}_{\mathrm{p}} = \mathbf{M}_{\nu,s}\left\{\mathbf{W}_{\nu,s}\mathbf{r}_{\mathrm{e}} + \left(\mathbf{I} - \mathbf{W}_{\nu,s}\right)\mathbf{r}_{\mathrm{a}}\right\} + \mathbf{b}_{\nu,s} + \boldsymbol{\epsilon}_{\nu,s}\ , \qquad (2)$$

where $\boldsymbol{\epsilon}_{\nu,s}$ is a new bivariate normal random variable, which depends on $\mathbf{M}_{\nu,s}$, $\mathbf{W}_{\nu,s}$, $\boldsymbol{\Sigma}_{\mathrm{a};\nu,s}$, $\boldsymbol{\Sigma}_{\mathrm{e};\nu,s}$, and $\boldsymbol{\epsilon}_{s}^{\mathrm{m}}$, and contains all response variability present in Equation 1.

Next, if an individual subject were actually performing a reliability-dependent MLE integration of stored egocentric and allocentric information about target location, then the weight

matrices in Equation 1 (and therefore 2) should be determined fully and uniquely by the variability inherent in estimates derived from these cues. In direct analogy with the well-known one dimensional case, the weighting of each cue would be given by

$$\mathbf{W}_{v,s} = \left(p_{v,s}^{-1}\boldsymbol{\Sigma}_{\mathrm{a};v,s}^{-1} + \boldsymbol{\Sigma}_{\mathrm{e};v,s}^{-1} \right)^{-1} \boldsymbol{\Sigma}_{\mathrm{e};v,s}^{-1}, \quad (3)$$

where the various symbols have the same meaning as above and $p_{v,s} = 1$. Finally, we assumed that landmark instability would affect the weight matrices in Equation 3 independently of the actual reliability of egocentric or allocentric information. We modeled this with the addition of the stability parameter, $p_{v,s}$, which was intended to represent the effects of a stability heuristic that modulates the apparent reliability of allocentric information based upon unstable landmarks. More specifically, if this parameter is greater than one, then it has the effect of making allocentric information look less reliable (more variable) in Equation 3 . Thus, for stable landmarks we take $p_{v,s} = 1$, while for unstable landmarks we have $p_{v,s} > 1$. This approach required fewer parameters than a fully Bayesian model with a prior.

If we wish to test the reliability-dependent MLE model defined by Equation 1 & Equation 3, then we need to find an estimate of $p_{v,s}$. This was accomplished by assuming that subjects were performing an MLE combination, and then using the predicted relationship between variability in the *three* experiments to determine uniquely the values for $\boldsymbol{\Sigma}_{\mathrm{a};v,s}$, $\boldsymbol{\Sigma}_{\mathrm{e};v,s}$, the motor noise covariance matrix and $p_{v,s}$. If the MLE assumption were in fact correct, then mean reaching endpoints in the cue-conflict experiment should be well-described by the combination of Equation 1 and Equation 3.

Model Fitting

After standard least-squares fitting to the raw endpoint dataset (no removal of systematic biases or transformation to allocentric weights, etc.), we used Equation 2 without the combined variability term to generate a set of predicted reaching endpoints for each subject in each condition. These calculated values were then transformed (as described above) into a corresponding set of allocentric weights, which we refer to here as *direct-fit allocentric weights.* Next, after determining estimates for $\boldsymbol{\Sigma}_{a;v,s}$, $\boldsymbol{\Sigma}_{e;v,s}$, the motor noise covariance matrix, and the stability parameter, $p_{v,s}$ from reaching endpoint variability (details in the Appendix), we replaced the directly fitted values of $\mathbf{W}_{v,s}$ in Equation 2 with the values from Equation 3. This allowed us to calculate the set of *MLE allocentric weights* for each subject in each experimental condition. If subjects really were performing an MLE combination of egocentric and allocentric information in the cue-conflict experiment, as we assumed, then the MLE allocentric weights should be identical to the direct-fit allocentric weights. In order to compare the between-subjects means for MLE and direct-fit allocentric weights in each experimental condition we performed a Bootstrapping procedure (see Appendix).

RESULTS

General Effect of landmark shift

Before examining the effects of reliability or the stability heuristic on cue-combination we first confirmed that both egocentric and allocentric information were being combined by subjects in the main cue-conflict experiment. If subjects were, indeed, relying on such a combination, then we would expect their reaching endpoints to satisfy two conditions. First, subjects should have touched on average a location *between* the original, egocentric target presentation location and the shifted, allocentric location. Such an effect can be seen for one example subject in Figure 4. The entire set of raw, target-relative reaching endpoints is divided into four panels according to

the quadrant direction of the landmark shift. For example, the upper left panel shows reaching endpoints (filled black circles) that followed landmark shifts to the upper-left quadrant of directions. Not surprisingly, the reaching endpoints here appear quite noisy, first because the scale is quite focused, and more fundamentally these endpoints are influenced by baseline noise, eye movement-induced noise (described above), and motor noise. However, the mean reaching endpoint (thick red circles) for this subject and for a given set of shift directions (i.e. upwards and to the left, upwards and to the right, etc.) was always shifted away from the original target location (origin) toward the line of allocentrically-defined locations (blue arcs). Hence, the landmark shift had a systematic effect in this subject.

In order to verify that subjects' reaching endpoints were, on average, between the egocentric and allocentric locations we first computed the mean allocentric weight for each subject in each experimental condition. Recall, the allocentric weight measure for a given reaching endpoint should be zero if a subject is using only egocentric information, or one if that subject is using only allocentric information. We found overall between-subjects allocentric weight means (±s.e.m.) of $M_{sv\_sgs} = 0.52 \pm 0.09$, $M_{sv\_lgs} = 0.44 \pm 0.09$, $M_{lv\_sgs} = 0.26 \pm 0.09$, and $M_{lv\_lgs} = 0.39 \pm 0.08$. For each experimental condition we compared the set of 10 subject means to zero, a purely egocentric response, and to one, a purely allocentric response. This set of eight comparisons was performed with standard t-tests, using the stepwise Holm-Bonferroni procedure to correct for multiple comparisons. All tests were found to be significant at the alpha = 0.05 level (comparison with zero: $p_{sv\_sgs} = 0.001$, $p_{sv\_lgs} = 0.002$, $p_{lv\_sgs} = 0.016$, $p_{lv\_lgs} = 0.002$; comparison with one: $p_{sv\_sgs} = 0.002$, $p_{sv\_lgs} = 0.0006$, $p_{lv\_sgs} = 0.0001$, $p_{lv\_lgs} = 0.0003$). Thus, in all conditions subjects touched a point between the original target location and the allocentric location, as expected if both cues were being used.

If subjects used visual landmarks as an allocentric cue, then their reaching endpoints should have also covaried with the location of the target relative to the landmarks. For any given trial in our task the location of the visual target relative to the centre of the landmark array (on its first presentation) should predict where the subject touches relative to the landmark array centre on its second presentation. In order to test this we regressed reaching endpoint relative to shifted landmark array centre against target location relative to the original landmark array centre for each subject in each condition. Horizontal and vertical components were regressed separately. This yielded a set of 20 correlation coefficients (two for each subject, one horizontal and one vertical) for each experimental condition. Between-subject means for correlation coefficients within each experimental condition were found to be significantly greater than zero (Holm-Bonferroni corrected *p*-values ranging from *0.001* to *0.013* after Fisher r-to-z transform), indicating that subjects were indeed using the visual landmarks as allocentric cues (all correlation coefficient values are presented in Supplementary Table S1).

The above results confirm that our subjects used both egocentric and allocentric information to different degrees, but they do not tell us how they weighted these factors to choose a particular reaching direction. To test this we had to examine how egocentric-allocentric weighting was affected by our stability and reliability manipulations (see methods). However, first we had to determine the exact effect these manipulations had on variable reaching errors so that we could parameterize our MLE model. Therefore, in the next three sections we present results from our two control experiments before returning to the cue-conflict experiment.

Effect of gaze amplitude in the egocentric control

One purpose of the egocentric-variability experiment was to test our assumption that the overall gaze trajectory length influences the amount of variability in memory-guided reaching endpoints

when only egocentric information is available. Any increase in variability, we assume, must be indicative of decreased reliability in maintained egocentric information. Raw, target-relative reaching endpoints are shown in Figure 5 for one typical subject. For this subject, reaching endpoints were more variable after large than after small gaze shifts. In fact, the overall reaching variance (defined above) was greater in the large versus small gaze-shift conditions for nine out of ten subjects, with between-subjects means of $M_{sgs} = 3.1 \pm 0.4 cm^2$ *and* $M_{lgs} = 5.3 \pm 1.3 cm^2$. *A priori* we would not expect overall reaching variance as defined here to be a normally distributed quantity. Therefore, we compared small and large gaze-shift conditions using a paired-samples Wilcoxon signed-rank test, yielding a significant difference across participants *($p = 0.012$).* Thus, the gaze-shift manipulation appears to have had the expected effect on egocentric information about target location. We will return to this dataset when we use it to predict weighting in our main cue-conflict experiment.

Effect of gaze amplitude in the allocentric control

One purpose of the allocentric-variability control experiment was to test our assumption that varying gaze-shift amplitudes had *no* effect on allocentric information about target location. In this experiment subjects could generate accurate reaching endpoints only by using allocentric information. To confirm that subjects actually were attempting to reach accurately to the correct landmark-relative target location, as opposed to simply using some other heuristic (e.g. reaching to where they last saw the centre of the landmark array), we performed the same regression procedure as we did in order to verify the use of allocentric information in the main cue-conflict experiment. If subjects were using the visual landmarks as an allocentric cue, then the regression slopes should have been *equal* to one (because, up to random noise and systematic offsets, the reaching endpoint on a given trial should have been equal to the original landmark-relative

location of the visual target). Between-subject means for correlation coefficients within each experimental condition were found to be significantly greater than zero for horizontal and vertical directions (Holm-Bonferroni corrected *p*-values ranging from *0.0002* to *0.006* after Fisher r-to-z transform), while regression slopes were not found to differ significantly from one *(p= 1* for all comparisons, except *p= 0.3* for the horizontal *sv_sgs* slope*)*, indicating that subjects were using the visual landmarks as an allocentric cue (all correlation coefficient and slope values are presented in Supplementary Table S1).

Sample raw, target-relative reaching data for one subject in the allocentric-variability control experiment is shown in Figure 6. Reaching endpoint variability for this subject appears to be similar in all conditions. In order to quantitatively examine the effect of gaze-shift amplitude on allocentric information across all subjects we calculated the overall reaching variance for each subject in each condition, giving between-subjects means of $M_{sv\_sgs} = 3.8 \pm 0.7 cm^2$, $M_{sv\_lgs} = 4.1 \pm 0.8 cm^2$, $M_{lv\_sgs} = 3.5 \pm 0.7 cm^2$, and $M_{lv\_lgs} = 3.7 \pm 0.6 \text{cm}^2$. Comparing the small and large gaze-shift means within each vibration amplitude condition revealed no significant difference within the small vibration condition *(Wilcoxon signed-rank, p = 0.13)* or within the large vibration amplitude condition *(Wilcoxon signed-rank, p = 0.49)*. Thus, varying gaze-shift amplitude did not appear to affect reliability of allocentric information about target location. Again, we will return to this data set when we use it to predict reaching endpoints in our cue-conflict experiment.

Effect of varying landmark vibration amplitude

Varying the vibration amplitude of the landmarks could have two effects. First, as per our intention, subjects might judge an unstable landmark to be less useful than a more stable landmark and place less weight on the former compared to the latter when combining this

information with egocentric information. Second, it could induce noise directly into the allocentric information for reaching, thereby decreasing allocentric reliability (as gaze did for egocentric information). To test this second possibility we compared the overall reaching variance within each gaze-shift amplitude condition of the allocentric-variability control experiment. No significant difference was found within either the small gaze-shift condition *(Wilcoxon signed-rank, $p = 0.49$)* or the large gaze-shift condition *(Wilcoxon signed-rank, $p = 1$)*. Thus, we were successful in varying landmark stability without influencing actual reliability in the allocentric channel. We will return to this dataset when we use it to predict weighting in our main cue-conflict experiment.

Weighting as a function of landmark stability and reliability

We hypothesized that subjects would place less weight on unstable landmarks relative to stable landmarks. Thus, even though landmark vibration amplitude appeared to have no effect on allocentric reliability, we still expected subjects to produce smaller allocentric weights for landmarks with high vibration amplitude (unstable) compared with the low amplitude vibration condition (stable). Given that larger gaze-shift amplitudes produced more egocentric reaching variability, but had no effect on allocentric reliability, we hypothesized that subjects would have generated relatively larger allocentric weights for larger gaze-shifts than for small ones. In order to test these predictions we performed a mixed-model ANOVA on the full set of allocentric weights, with gaze-shift amplitude and landmark vibration amplitude as two, two-level fixed factors, and subject ID as a random factor.

In Figure 3B, the set of allocentric weights from all trials was divided into four bins for each subject according to the corresponding landmark shift direction (up and to the left, up and to the right, down and to the right, down and to the left) and the means for each direction bin

were averaged over subjects. Individual subjects showed quite variable allocentric weightings, with inter-subject variance confirmed to be a significant factor in the data *(F(9,4.57) = 7.21, p = 0.027)*, and with allocentric weight means for individual subjects ranging from 0.21 to 0.90 (see Supplementary Figure S2 for a direction-dependent breakdown of individual subject allocentric weights).

In Figure 7, the mean allocentric weights are plotted as a function of landmark shift direction, with data separated according to vibration amplitude in the upper circle and data separated according to gaze shift amplitude in the lower circle. From the upper panel it appears as though landmarks with a small vibration amplitude (red curve) had a larger effect on reaching endpoints than did landmarks with a large vibration amplitude (blue curve), especially along a tilted vertical axis. This main effect of landmark vibration amplitude was found to be significant *(F(1,9.83) = 6.2, p = 0.032)*, with the mean between-subjects allocentric weight for large vibration amplitude trials being 0.48 as compared to a mean of 0.33 for the small amplitude vibration trials, but no main effect of gaze-shift amplitude. Thus, visual vibration had the only clear effect on the weighting of allocentric information.

Returning to our original model, we used only raw reaching endpoint variability from the main and control experiments in an optimization procedure to derive estimates of egocentric and allocentric reliability, of motor noise, *and of the stability parameter,* $p_{v,s}$ (see Appendix). These estimates allowed us to substitute the weight matrices in Equation 2 with MLE estimates from Equation 3 to produce the set of MLE allocentric weights. The results of this procedure are shown in Figure 8. Our model clearly predicted that allocentric information derived from unstable landmarks would be weighed less by subjects in egocentric-allocentric combination than would those derived from stable landmarks, even though stable and unstable landmarks

resulted in similar allocentric reliabilities. This pattern is consistent with the measured data described above.

To analyze our data in a more quantitative fashion, we fit the model embodied in Equation 2 to the raw reaching endpoints measured in the main cue-conflict experiment. Calculating direct-fit allocentric weights from this model (as described above) also produced trends that were qualitatively and quantitatively similar to the MLE allocentric weights (see Figure 8). A simple Bootstrap (see Appendix) procedure revealed no statistical difference between the direct-fit allocentric weights and the corresponding MLE allocentric weight predictions. We also tested if our model was able to reproduce specific allocentric weights corresponding to different landmark shift directions (e.g. van Beers et al. 1999). To do this, we calculated direct-fit and MLE allocentric weights as above, but averaged them separately for each full quadrant of shift directions. The model results agreed well with the quadrant-specific effects observed in the experimental data (Supplementary Figure S3).

In order to verify the importance of the stability parameter, we recalculated the MLE allocentric weights under the constraint that $p_{v,s} = 1$ for all conditions. The resulting allocentric weight predictions are also depicted in Figure 8, with the Bootstrapping procedure revealing significant differences between the predictions of this reduced model and the actual data. Thus, allowing a value of $p_{v,s}$ greater than one (i.e. allowing for a reduced reliance on unstable landmarks regardless of actual reliability) was essential to accurately predicting the empirical data.

DISCUSSION

Performance in egocentric and allocentric controls

Our control results confirm that subjects were able to reach to remembered targets with reasonable accuracy based on either egocentric or allocentric cues in isolation. This is demonstrated by the fact that between-subjects means for our measure of variable error were at most a little over five square centimeters for any of our control experiments -- small compared with the area over which target location varied. Furthermore, in the allocentric-variability control experiment reaching endpoints within the final landmark array were strongly correlated with target location within the original array, supporting our assumption that subjects would use the landmarks in the intended way.

In comparison with other experiments that involve open-loop reaches to remembered targets, endpoint variability in our task was substantially larger than that measured in some experiments (e.g. Krigolson and Heath 2004), but smaller than that measured in others (e.g. Lemay et al. 2004). In addition, Lemay et al. have found that reaches based solely on allocentric information tend to be less variable than reaches based solely on egocentric information. We found no such difference in our results, but our paradigm was also different in numerous aspects. The relative similarity in endpoint variability we found between egocentric and allocentric tasks is consistent with the roughly equal weighting we found between egocentric and allocentric cues in the cue-conflict experiment (see next section).

Perhaps more importantly, within our egocentric-variability control experiment we found that larger gaze-shifts during the memory delay induced more variability in reaching endpoints, confirming one assumption behind our experimental design (Prime et al. 2007). This finding is consistent with the idea that egocentric representations of target location are continuously updated each time the eyes move (Henriques et al. 1998; Khan et al. 2005a; Khan et al. 2005b; Medendorp and Crawford 2002; Medendorp et al. 2003b; Merriam et al. 2003). In contrast, in

the allocentric-variability control results we found that gaze-shift amplitude had no effect on reach variability, consistent with the general assumption that landmark-relative representations are likely useful because they do not vary with the orientation or configuration of the self in space (e.g. Burgess 2006). The fact that landmark vibration amplitude had little effect on reaching variability in the allocentric task was unexpected, but fortuitous - it meant we were primarily manipulating landmark stability without affecting the reliability of allocentric information and could attribute any change in weighting to the stability heuristic. Each of these factors was then accounted for in our MLE analysis of the cue-conflict experiment, central to the main goals of the experiment.

Weighting of egocentric and allocentric factors in the cue-conflict experiment

As predicted by our MLE model, the shifting visual landmarks in our experiment tended to draw subjects' reaching responses away from the original target location and towards the allocentric location. Although the weighting factor varied considerably across subjects, both the model predictions and empirical data indicated an overall average weighting of approximately 60% egocentric and 40% allocentric. In some respects it is surprising that allocentric cues had this much effect on reaching, because in debriefing sessions after the cue-conflict experiment subjects indicated that they sometimes detected the allocentric shifts. Indeed, Kording et al. (2007) show that judgments about a target's perceived location can be heavily influenced by whether a visual cue and an auditory cue to that target's actual location are perceived as coming from a common source or two separate sources. Given that our MLE model well reproduces our data, this suggests that the weighting of allocentric cues is either hardwired into the visuomotor system or independent of conscious awareness.

We cannot rule out the possibility that allocentric weighting in our experiment would have been even higher if the shifts were not at all detectible, but this was not possible to test in our design because it would require cue-shifts to be too small to produce statistical effects against the background noise in our subjects' performance. We also cannot rule out the possibility that our instructions (ignore the blue dots) did not lessen the effect of the shifting landmarks. Furthermore, Dassonville and Bala (2004) have shown that pointing to egocentric targets can be influenced by an "off-centre" frame that shifts the subject's estimate of straight ahead. Our frame was much smaller than that of Dassonville & Bala, and other interpretations of their results exist: e.g. de Grave et al. (2002). But in principle, this effect could have produced or influenced the overall shift results we found. However, given the good agreement between our MLE model and our data in all four experimental conditions, and even across shift directions (Supplementary Figure S3), we believe that we have provided strong support for our hypothesis: that humans can and do combine egocentric and allocentric cues to reach toward remembered targets. This finding underscores the brain's ability to draw upon multiple available information sources when generating behavior, as opposed to simply following some fixed strategy in which only a subset of relevant stimulus information is used in any given context.

Our model predicted a main effect of landmark stability on mean reaching endpoints that was in quantitative agreement with the empirically observed value. Thus, egocentric and allocentric visual information appear to be combined by the brain in a stimulus-dependent fashion when generating reaching responses to remembered targets. The fact that a reduced version of our model, one with no stability parameter, could not account for this finding confirms our second hypothesis: that human subjects use heuristic information beyond actual reliability when combining egocentric and allocentric information.

Here, our work extends the results of Burgess et al.(2004). These authors had subjects pick which object out of an array of previously viewed objects had been covertly shifted during a brief delay period in which the subject was blindfolded. During this delay, a variety of manipulations could have occurred, including rotation of the circular table on which the objects lay, displacement of an external visual landmark (not on the table), or displacement of the subject via guided walking to a new location around the table. Of relevance here, performance was found to be higher for stationary table/stationary landmark conditions (conditions in which the landmark could be useful) when subjects had not yet been exposed to trials in which the external landmark shifted location between presentation and test (i.e. they seemed to rely more heavily on the landmark when it was thought to be stable). In our work we go further by explicitly examining the cue-combination question and MLE weighting predictions. However, subjects in the Burgess et al. task were likely down-weighting allocentric information because of their past experience with the landmark on previous trial of the experiment. This is not the case in our experiment because the landmarks were equally useful regardless of stability and, therefore, subjects should not have learned to down-weight them. Thus, our subjects must have learned previously or have been hardwired to assume moving landmarks would be less useful.

If one only considers performance within the confines of an impoverished laboratory enviroment, this implementation by the brain of a stability heuristic is not optimal behavior. This is because (as we showed) the large amplitude vibration of the cue did not degrade reaching responses. However, the stability parameter in our model was based on the assumption that in natural settings a stability heuristic *might* actually be optimal. In nature, landmark motion cannot be assumed to result from vibration in one place, but instead is more likely to be motion that would interrupt its validity as a spatial cue, and/or would require extensive temporal averaging to

cancel. Thus, our data were consistent with this hypothesis, and from this broader perspective it appears that our subjects' performance was optimized for behavior in natural, unpredictable settings.

Unexpectedly, we did not find any changes in cue weighting when we varied gaze path length (and thus egocentric reliability) during the memory delay. At first glance, this result appeared (even to us) not only counter-intuitive, but to contradict the predictions of our egocentric-variability control experiment in which reaching variability increased by 42% between small and large gaze shift conditions. Based on this, we expected to see a marked difference in cue weighting in these two versions of our cue-conflict experiment. However, this intuition proved false when the data were quantitatively tested against a full MLE model. In brief, the reason is that our initial intuitions were based on a one-dimensional approximation to an inherently two-dimensional quantity. As indicated by the results from our full MLE model, the predicted difference for large versus small gaze-shifts (bottom panel of Figure 8) was simply too small for us to detect in this data set. In general, these results highlight the difficulty of making intuitive predictions when several different interacting factors are at play: quantitative models are required. However, the good agreement between our full MLE model and the data confirms our third hypothesis: that egocentric and allocentric information appear to be combined in a reliability-dependent fashion.

Comparison to Previous Cue-Combination Studies

As discussed in the introduction, numerous studies have investigated the factors that influence egocentric-allocentric combination for reaching. However, few if any have actually examined the role that intrinsic stimulus properties play in the underlying combination rule. By showing that a

812 reliability-dependent MLE model could account quantitatively for our results we have provided
813 further support for the idea that the brain generally combines information in a statistically
814 optimal fashion. However, we have also shown that additional stimulus properties which do not
815 necessarily influence cue reliability must also be taken into account in order to understand fully
816 the cue-combination process that allows for a motor response. We emphasize the motor nature of
817 our task because Knill (2005) has shown that the details of cue-combination do indeed vary
818 based upon whether a response is motor or perceptual. Thus, our findings might not generalize to
819 the latter domain.

820 Of course, it is possible that additional variables that we did not explicitly consider may
821 have contributed to endpoint variability and egocentric-allocentric weighting in our task. For
822 example, movement times and other kinematic variables are often found to correlate in some
823 way with the final reaching endpoints in tasks similar to ours (Heath et al. 2008). Including some
824 of these variables in our model may have further improved the resulting fits, but since our fits are
825 already quite good, we assume that these extra variables do not contain much additional
826 information in our case.

827 Although we found good agreement between our experimental results and our
828 stability/reliability-dependent MLE model, a full Bayesian model would allow for the influence
829 of multiple prior probabilities on various stimulus-related and internally-generated quantities. It
830 has been found in both perceptual (Knill 2007a) and motor (Kording and Wolpert 2004) tasks
831 that the brain does often operate on such Bayesian principles. Thus, it might be interesting to see
832 if subjects could be trained to rely more heavily on the *unstable* landmarks in our experiment.
833 This might be accomplished by providing trial-to-trial feedback on reaching performance such
834 that subjects were led to believe that their responses were more accurate in the presence of the

unstable landmarks. Finding such a reversal in behaviour would constitute an excellent demonstration that the brain does rely on Bayesian principles when combining egocentric and allocentric information about reaching target location.

Aside from the stability/reliability-dependent effects seen in our experiment, the fact that subjects could not ignore the visual landmarks even though they were instructed explicitly to do so —a seemingly simple task given that most subjects claimed in a debriefing session after the experiment to have subjectively detected the shift on at least some of the trials— is interesting in itself. Such a finding is consistent with an action-perception dissociation (Goodale and Milner 1992). Moreover, this inability to ignore allocentric information could have numerous practical and experimental implications (e.g., in a room that is not completely dark, even barely visible visual geometric information might still be used by the brain and influence results).

Another seemingly innocuous stimulus is a fixation point used for gaze position. If not extinguished at the right time, this allocentric cue could influence the behavioral response. For example, reach tends to be biased toward the nearest irrelevant landmark (Diedrichsen et al. 2004). This could affect numerous studies, so we will just highlight one relevant example. When humans point or reach toward objects that are not aligned with gaze, the hand tends to overshoot relative to gaze (Bock 1986). This is thought to arise from some unknown error in the visual-motor transformation (Beurze et al. 2006; Henriques et al. 1998). McGuire and Sabes (2009) modeled this by incorporating a mis-estimate of gaze direction relative to the desired reach direction, as well as several other features. The model was successful at independently reproducing most of their experimental data, but it overestimated the effect for larger retinal eccentricities (their Figure 5). However, their continuously illuminated fixation light may have had a distance-dependent influence on performance (Diedrichsen et al. 2004) that was not

858 accounted for in the model. Removal of the fixation point at the time of reaching, might have
859 improved the fits between their model and their data.
860
861 *Possible Physiological Mechanisms*
862 The neural mechanisms underlying reaching based upon egocentric and allocentric cues remain
863 elusive. Since Goodale and Milner introduced their influential action-perception model posterior
864 parietal regions in the so-called dorsal visual stream have become strongly associated with
865 visually-guided action, while temporal regions in the ventral stream have become associated with
866 visual perception. However, delayed action based on remembered targets has also been argued to
867 depend on the ventral stream (Goodale et al. 2004). Moreover, various emerging lines of
868 evidence suggest that the dorsal stream processes egocentric visuospatial information, while the
869 ventral stream deals more with allocentric information - whether for action *or* perception (Carey
870 et al. 2006; Schenk 2006). In line with this idea, Thaler and Todd (2009) have shown that the
871 specific reference frame (egocentric or allocentric) used for a task affects response variance, but
872 that such variance is unaffected by whether the task is related to action or perception. Other
873 experiments suggest that egocentric and allocentric signals appear in both streams. For example,
874 neurons in the lateral intraparietal area of the monkey show rudimentary feature responses
875 (Sereno and Maunsell 1998). However, it appears that highly detailed object-relative spatial
876 information is represented in ventrolateral temporo-occipital areas comprising the ventral stream
877 (Brincat and Connor 2004; Pasupathy and Connor 2002).
878 Assuming that the initial detailed analysis of allocentric information is performed in the
879 ventral visual stream, it still must enter the 'dorsal stream' parieto-frontal loop at some point to
880 influence motor behavior. Consistent with this, egocentric *and* allocentric judgment tasks have

been shown to produce elevated levels of activity in the right human posterior parietal cortex (Galati et al. 2000; Zaehle et al. 2007). In addition, monkeys trained to perform visuospatial tasks involving both egocentic and allocentric elements showed clear object-centered neural responses in pre-frontal cortex (Olson and Tremblay 2000) and in posterior parietal cortex (Chafee et al. 2007; Crowe et al. 2008; Sabes et al. 2002). Interestingly, Crowe et al.'s results suggest that egocentric representations of target location are formed in parietal cortex (specifically area 7a) before object-based ones. This could imply that the egocentric representations are being transformed into allocentric ones in parietal cortex or that the allocentric information is arriving there from elsewhere, possibly from ventral stream regions, as we describe below.

The possibility that object-based allocentric information flows from the ventral visual stream to posterior parietal cortex is similar to the principle underlying a neural network model proposed by Byrne et al. (2007). Within this model, landmark-based allocentric representations of navigable space are initially found in medial temporal areas but must be transformed into egocentric representations via posterior parietal cortex in order to be used for path planning, mental imagery, etc (for a review of evidence supporting this principle, see Vann et al. (2009)). Indeed, Committeri et al. (2004) have shown that egocentric, landmark-based allocentric, and object-based allocentric tasks all produced activation in parieto-frontal areas, while landmark-based allocentric tasks produced activation in ventromedial temporal areas, and object-based allocentric tasks produced activation in ventrolateral areas of temporal and occipital cortices. Hence, we speculate that object-based allocentric representations in our task were initially formed in the ventral visual stream and then transferred to the parieto-frontal loop for visuomotor control via posterior parietal regions. This transfer could occur directly, or via reciprocal

recurrent connections between the dorsal stream and the ventral stream at the level of occipital cortex (Merriam et al. 2007; Prime et al. 2008).

Once allocentric information enters the parieto-frontal loop, it might either be combined immediately with egocentric information to generate a single representation of target location that is maintained over memory delays, or it might be maintained there separately until a reaching response is required. Whichever the case, numerous studies indicate that a dorsolateral prefrontal cortex-posterior parietal cortex loop is essential in the maintenance of spatial memory in a wide variety of working memory tasks (e.g. Chafee and Goldman-Rakic 1998; Koch et al. 2005). In the case of saccade targets both egocentric (Dassonville et al. 1992; Schlag and Schlag-Rey 1987; Thier and Andersen 1998, 1996) and allocentric (Olson and Gettner 1995; Sabes et al. 2002) representations of target location have been found in the parieto-frontal loop. In the case of reaching targets a region of human parietal cortex, tentatively referred to as human PRR, has been shown to support gaze-centered (i.e. egocentric) representations of reach target location during memory intervals (Medendorp et al. 2003a). However, to our knowledge allocentric representations of reach target location have not been found in parieto-frontal circuitry (but see Snyder et al. 1998), so it is difficult to comment with any more certainty.

Another question is the physiological mechanism for the stability heuristic used in our model. It is likely in our experiment that cue vibration was detected by the MT/MST complex, which is exquisitely sensitive to visual motion and projects to both parietal and frontal movement areas (eg. Ilg 2008). But again, it is highly uncertain where this information enters the parieto-frontal loop. One speculative possibility is that egocentric and allocentric representations of target location are integrated in premotor cortex. This is suggested by the work of Verhagen et al.

926 (2008) who show that the ventral premotor region seems to be involved in integrating perceptual
927 information from the ventral stream into the grasp plan.
928
929 *Conclusions*
930 In summary, we have provided the first demonstration using a cue-conflict paradigm that
931 egocentric and allocentric visual information are combined in a stimulus-dependent fashion for
932 generating reaching movements to visual targets. Perhaps most importantly, we have shown that
933 the underlying combination rule seems to depend on heuristics beyond an accounting for actual
934 cue reliability. This finding is important because it shows that although the brain can make
935 intelligent use of the various sources of information that are available to it, it might also depend
936 to an extent on certain inflexible "rules of thumb". We have also shown that the underlying
937 combination process, whatever its exact nature, is obligatory and cannot easily be overridden by
938 conscious processes based on perception.
939
940
941
942
943 APPENDIX
944
945 In order to calculate estimates for covariance matrices representing egocentric and allocentric
946 reliability and motor noise, and an estimate of the stability parameter, $p_{v,s}$, we first assumed that
947 subjects in the two variability control experiments based their reaching responses on similar
948 estimates as they did in the main experiment. Thus, a reaching endpoint in the allocentric-
949 variability experiment would be given by

950 $$\mathbf{r}_{\mathrm{p}}^{\mathrm{a}} = \mathbf{M}_{v,s}^{\mathrm{a}} \hat{\mathbf{r}}_{\mathrm{a};v,s}^{\mathrm{a}} + \mathbf{b}_{v,s}^{\mathrm{a}} + \boldsymbol{\epsilon}_{s}^{\mathrm{m}} \quad , \qquad (4)$$

where symbols have similar meanings as in Equations 1 & 2, and ν has an identical meaning because the same experimental conditions were used in the allocentric-variability control as in the main experiment. The superscript 'a' is used on some of the variables in Equation 4 to indicate that their values are not necessarily the same as the equivalent variables in Equations 1 & 2. Also, since subjects were exposed to identical reliability manipulations and stimulus characteristics in the allocentric-variability control experiment as in the main experiment, we assumed that $\hat{\mathbf{r}}^{\mathrm{a}}_{\mathrm{a};\nu,s}$ had the same covariance as allocentric information in the main experiment, namely $\boldsymbol{\Sigma}_{\mathrm{a};\nu,s}$. For the egocentric-variability control experiment, we have

$$\mathbf{r}^{\mathrm{e}}_{\mathrm{p}} = \mathbf{M}^{\mathrm{e}}_{\nu,s}\hat{\mathbf{r}}^{\mathrm{e}}_{\mathrm{e};\nu,s} + \mathbf{b}^{\mathrm{e}}_{\nu,s} + \boldsymbol{\epsilon}^{\mathrm{m}}_{s} \quad , \tag{5}$$

where ν refers only to small versus large gaze shifts since there were no landmarks in this control experiment. However, we did assume that $\hat{\mathbf{r}}^{\mathrm{e}}_{\mathrm{e};\nu,s}$ was distributed with the same covariance as egocentric information in the main experiment. That is, we assumed that $\boldsymbol{\Sigma}_{\mathrm{e};sv\_sgs,s}$ and $\boldsymbol{\Sigma}_{\mathrm{e};lv\_sgs,s}$ from the main experiment were equal to $\boldsymbol{\Sigma}_{\mathrm{e};sgs,s}$ from the control experiment, and similarly for the *sv_lgs* and *lv_lgs* conditions. Hence, we also refer to the covariance of $\hat{\mathbf{r}}^{\mathrm{e}}_{\mathrm{e};\nu,s}$ as $\boldsymbol{\Sigma}_{\mathrm{e};\nu,s}$.

Rewriting Equations 4 & 5 in the same way that we converted Equation 1 into Equation 2 gives

$$\mathbf{r}^{\mathrm{a}}_{\mathrm{p}} = \mathbf{M}^{\mathrm{a}}_{\nu,s}\mathbf{r}^{\mathrm{a}}_{\mathrm{a}} + \mathbf{b}^{\mathrm{a}}_{\nu,s} + \boldsymbol{\epsilon}^{\mathrm{a}}_{\nu,s}, \tag{6}$$

and

$$\mathbf{r}^{\mathrm{e}}_{\mathrm{p}} = \mathbf{M}^{\mathrm{e}}_{\nu,s}\mathbf{r}^{\mathrm{e}}_{\mathrm{e}} + \mathbf{b}^{\mathrm{e}}_{\nu,s} + \boldsymbol{\epsilon}^{\mathrm{e}}_{\nu,s}. \tag{7}$$

Fitting Equations 2, 6, and 7 yielded a set of residuals for each subject and each condition in each experiment. We denote the covariance matrices corresponding to residuals from the main cue-conflict, the allocentric-variability control, and the egocentric-variability control experiments by $\mathbf{C}_{v,s}$, $\mathbf{C}^{\mathrm{a}}_{v,s}$, and $\mathbf{C}^{\mathrm{e}}_{v,s}$ respectively. From the right hand sides of Equations 1, 4, and 5 we calculated the expected values of these covariances, giving

$$\mathbf{C}_{v,s} = \mathbf{M}_{v,s}\mathbf{W}_{v,s}\boldsymbol{\Sigma}_{\mathrm{e};v,s}\left(\mathbf{M}_{v,s}\mathbf{W}_{v,s}\right)^{\mathrm{T}} + \mathbf{M}_{v,s}\left(\mathbf{I}-\mathbf{W}_{v,s}\right)\boldsymbol{\Sigma}_{\mathrm{a};v,s}\left(\mathbf{M}_{v,s}\left(\mathbf{I}-\mathbf{W}_{v,s}\right)\right)^{\mathrm{T}} + \boldsymbol{\Sigma}^{\mathrm{m}}_{s}, \quad (8)$$

$$\mathbf{C}^{\mathrm{a}}_{v,s} = \mathbf{M}^{\mathrm{a}}_{v,s}\boldsymbol{\Sigma}_{\mathrm{a};v,s}\left(\mathbf{M}^{\mathrm{a}}_{v,s}\right)^{\mathrm{T}} + \boldsymbol{\Sigma}^{\mathrm{m}}_{s}, \quad (9)$$

and

$$\mathbf{C}^{\mathrm{e}}_{v,s} = \mathbf{M}^{\mathrm{e}}_{v,s}\boldsymbol{\Sigma}_{\mathrm{e};v,s}\left(\mathbf{M}^{\mathrm{e}}_{v,s}\right)^{\mathrm{T}} + \boldsymbol{\Sigma}^{\mathrm{m}}_{s}, \quad (10)$$

where the superscript T is matrix transpose and $\mathbf{I}$ is the identity matrix.

Were it not for motor error we could simply use Equations 9 & 10 to solve for $\boldsymbol{\Sigma}_{\mathrm{a};v,s}$ and $\boldsymbol{\Sigma}_{\mathrm{e};v,s}$ in the main experiment. However, we require an estimate for $\boldsymbol{\Sigma}^{\mathrm{m}}_{s}$ and for the stability parameter. We obtained this by *presupposing* that subjects were using a reliability-dependent MLE combination of egocentric and allocentric information. By doing this we could solve Equations 9 & 10 for $\boldsymbol{\Sigma}_{\mathrm{a};v,s}$ and $\boldsymbol{\Sigma}_{\mathrm{e};v,s}$, substitute these values into Equation 3 & 8, and then substitute Equation 3 into Equation 8. This yielded a set of four two-by-two matrix Equations of the form

$$\mathbf{F}_{v}\left(\boldsymbol{\Sigma}^{\mathrm{m}}_{s}, p_{v,s}\right) = \mathbf{0}, \quad (11)$$

where $\mathbf{F}_v$ is a matrix function depending on experimental condition. Thus, in order to find an estimate of $\boldsymbol{\Sigma}_s^{\mathrm{m}}$, we numerically minimized the objective function,

$$\sum_{v}\sum_{i,j}\left[F_{v_{i,j}}\left(\boldsymbol{\Sigma}_s^{\mathrm{m}}, p_{v,s}\right)\right]^2, \tag{12}$$

with respect to $p_{lv\_sgs,s} = p_{lv\_lgs,s,} = p_s$ and the components of $\boldsymbol{\Sigma}_s^{\mathrm{m}}$. Note, as describe above we have taken $p_{v,s} = 1$ for both small vibration, stable landmark conditions.

Once we obtained estimates of $\boldsymbol{\Sigma}_s^{\mathrm{m}}$ and $p_{v,s}$ for each subject, we used Equations 9 and 10 to calculate $\boldsymbol{\Sigma}_{\mathrm{a};v,s}$ and $\boldsymbol{\Sigma}_{\mathrm{e};v,s}$ for each subject in each condition. These values were then used with Equation 3 to generate weight matrices for Equation 2. As described in the Methods sections, we then used Equation 2 to produce the set of MLE allocentric weights. The entire optimization procedure, including the calculation of $\boldsymbol{\Sigma}_{\mathrm{a};v,s}$ and $\boldsymbol{\Sigma}_{\mathrm{e};v,s}$ was performed under the constraint that $\boldsymbol{\Sigma}_s^{\mathrm{m}}$, $\boldsymbol{\Sigma}_{\mathrm{a};v,s}$, and $\boldsymbol{\Sigma}_{\mathrm{e};v,s}$ had to be real, symmetric and positive definite (i.e. they had to be valid covariance matrices).

In order to generate confidence intervals for the differences between the MLE allocentric weights and the direct-fit weights in each experimental condition we first calculated the difference between each individual subject's MLE and direct-fit mean in that condition. We then re-sampled this set of differences (with replacement) 10000 times and to produce 95% confidence intervals for the mean MLE/direct-fit allocentric weight difference in each condition. This procedure revealed no significant differences between our model and the data.

In order to investigate the importance of the stability parameter, we set $p_{lv\_sgs,s} = p_{lv\_lgs,s,} = 1$ in Equation 3 so that only the components of $\boldsymbol{\Sigma}_s^{\mathrm{m}}$ varied in Equation 12. Bootstrapping was

performed for this reduced model in an identical fashion to the full model, revealing significant differences between MLE and direct-fit allocentric weights.

ACKNOWLEDGMENTS

This research was supported by a grant from the Canadian Institutes of Health Research (CIHR). Pat Byrne was supported by the CIHR Strategic Training Program in Vision Health Research. Doug Crawford was supported by a CIHR Canada Research Chair.

REFERENCES

Allen DM. Relationship between Variable Selection and Data Augmentation and a Method for Prediction. *Technometrics* 16: 125-127, 1974.

Ariff G, Donchin O, Nanayakkara T, and Shadmehr R. A real-time state predictor in motor control: study of saccadic eye movements during unseen reaching movements. *J Neurosci* 22: 7721-7729, 2002.

Batista AP, Buneo CA, Snyder LH, and Andersen RA. Reach plans in eye-centered coordinates. *Science* 285: 257-260, 1999.

Battaglia PW, Jacobs RA, and Aslin RN. Bayesian integration of visual and auditory signals for spatial localization. *J Opt Soc Am A Opt Image Sci Vis* 20: 1391-1397, 2003.

Beurze SM, Van Pelt S, and Medendorp WP. Behavioral reference frames for planning human reaching movements. *J Neurophysiol* 96: 352-362, 2006.

Biegler R and Morris R. Landmark stability: studies exploring whether the perceived stability of the environment influences spatial representation. *J Exp Biol* 199: 187-193, 1996a.

Biegler R and Morris RG. Landmark stability is a prerequisite for spatial but not discrimination learning. *Nature* 361: 631-633, 1993.

Biegler R and Morris RG. Landmark stability: further studies pointing to a role in spatial learning. *Q J Exp Psychol B* 49: 307-345, 1996b.

Blohm G and Crawford JD. Computations for geometrically accurate visually guided reaching in 3-D space. *J Vis* 7: 4 1-22, 2007.

Bock O. Contribution of retinal versus extraretinal signals towards visual localization in goal-directed movements. *Exp Brain Res* 64: 476-482, 1986.

Brainard DH. The Psychophysics Toolbox. *Spat Vis* 10: 433-436, 1997.

Bridgeman B, Peery S, and Anand S. Interaction of cognitive and sensorimotor maps of visual space. *Percept Psychophys* 59: 456-469, 1997.

Brincat SL and Connor CE. Underlying principles of visual shape selectivity in posterior inferotemporal cortex. *Nat Neurosci* 7: 880-886, 2004.

Brouwer AM and Knill DC. Humans use visual and remembered information about object location to plan pointing movements. *J Vis* 9: 24 21-19, 2009.

Buneo CA, Jarvis MR, Batista AP, and Andersen RA. Direct visuomotor transformations for reaching. *Nature* 416: 632-636, 2002.

Burgess N. Spatial memory: how egocentric and allocentric combine. *Trends Cogn Sci* 10: 551-557, 2006.

Burgess N, Spiers HJ, and Paleologou E. Orientational manoeuvres in the dark: dissociating allocentric and egocentric influences on spatial memory. *Cognition* 94: 149-166, 2004.

Byrne P, Becker S, and Burgess N. Remembering the past and imagining the future: a neural model of spatial memory and imagery. *Psychol Rev* 114: 340-375, 2007.

Carey DP, Dijkerman HC, Murphy KJ, Goodale MA, and Milner AD. Pointing to places and spaces in a patient with visual form agnosia. *Neuropsychologia* 44: 1584-1594, 2006.

Carlton LG. Processing visual feedback information for movement control. *J Exp Psychol Hum Percept Perform* 7: 1019-1030, 1981.

Carrozzo M, Stratta F, McIntyre J, and Lacquaniti F. Cognitive allocentric representations of visual space shape pointing errors. *Exp Brain Res* 147: 426-436, 2002.

1095 **Chafee MV, Averbeck BB, and Crowe DA**. Representing spatial relationships in posterior
1096 parietal cortex: single neurons code object-referenced position. *Cereb Cortex* 17: 2914-2932,
1097 2007.
1098 **Chafee MV and Goldman-Rakic PS**. Matching patterns of activity in primate prefrontal area 8a
1099 and parietal area 7ip neurons during a spatial working memory task. *J Neurophysiol* 79: 2919-
1100 2940, 1998.
1101 **Committeri G, Galati G, Paradis AL, Pizzamiglio L, Berthoz A, and LeBihan D**. Reference
1102 frames for spatial cognition: different brain areas are involved in viewer-, object-, and landmark-
1103 centered judgments about object location. *J Cogn Neurosci* 16: 1517-1535, 2004.
1104 **Crawford JD, Medendorp WP, and Marotta JJ**. Spatial transformations for eye-hand
1105 coordination. *J Neurophysiol* 92: 10-19, 2004.
1106 **Crowe DA, Averbeck BB, and Chafee MV**. Neural ensemble decoding reveals a correlate of
1107 viewer- to object-centered spatial transformation in monkey parietal cortex. *J Neurosci* 28: 5218-
1108 5228, 2008.
1109 **Dassonville P and Bala JK**. Perception, action, and Roelofs effect: a mere illusion of
1110 dissociation. *PLoS Biol* 2: e364, 2004.
1111 **Dassonville P, Schlag J, and Schlag-Rey M**. The frontal eye field provides the goal of saccadic
1112 eye movement. *Exp Brain Res* 89: 300-310, 1992.
1113 **de Grave DD, Brenner E, and Smeets JB**. Are the original Roelofs effect and the induced
1114 Roelofs effect caused by the same shift in straight ahead? *Vision Res* 42: 2279-2285, 2002.
1115 **de Grave DD, Brenner E, and Smeets JB**. Illusions as a tool to study the coding of pointing
1116 movements. *Exp Brain Res* 155: 56-62, 2004.
1117 **Diedrichsen J, Werner S, Schmidt T, and Trommershauser J**. Immediate spatial distortions
1118 of pointing movements induced by visual landmarks. *Percept Psychophys* 66: 89-103, 2004.
1119 **Ernst MO and Banks MS**. Humans integrate visual and haptic information in a statistically
1120 optimal fashion. *Nature* 415: 429-433, 2002.
1121 **Flanagan JR, King S, Wolpert DM, and Johansson RS**. Sensorimotor prediction and memory
1122 in object manipulation. *Can J Exp Psychol* 55: 87-95, 2001.
1123 **Flanagan JR, Terao Y, and Johansson RS**. Gaze behavior when reaching to remembered
1124 targets. *J Neurophysiol* 100: 1533-1543, 2008.
1125 **Flanagan JR, Vetter P, Johansson RS, and Wolpert DM**. Prediction precedes control in motor
1126 learning. *Curr Biol* 13: 146-150, 2003.
1127 **Galati G, Lobel E, Vallar G, Berthoz A, Pizzamiglio L, and Le Bihan D**. The neural basis of
1128 egocentric and allocentric coding of space in humans: a functional magnetic resonance study.
1129 *Exp Brain Res* 133: 156-164, 2000.
1130 **Glover S and Dixon P**. A step and a hop on the Muller-Lyer: illusion effects on lower-limb
1131 movements. *Exp Brain Res* 154: 504-512, 2004.
1132 **Goodale MA and Milner AD**. Separate visual pathways for perception and action. *Trends*
1133 *Neurosci* 15: 20-25, 1992.
1134 **Goodale MA, Westwood DA, and Milner AD**. Two distinct modes of control for object-
1135 directed action. *Prog Brain Res* 144: 131-144, 2004.
1136 **Hanisch C, Konczak J, and Dohle C**. The effect of the Ebbinghaus illusion on grasping
1137 behaviour of children. *Exp Brain Res* 137: 237-245, 2001.
1138 **Hay L and Redon C**. Response delay and spatial representation in pointing movements.
1139 *Neurosci Lett* 408: 194-198, 2006.

1140 **Heath M, Maraj A, Godbolt B, and Binsted G**. Action without awareness: reaching to an
1141 object you do not remember seeing. *PLoS One* 3: e3539, 2008.
1142 **Henriques DY, Klier EM, Smith MA, Lowy D, and Crawford JD**. Gaze-centered remapping
1143 of remembered visual space in an open-loop pointing task. *J Neurosci* 18: 1583-1594, 1998.
1144 **Ilg UJ**. The role of areas MT and MST in coding of visual motion underlying the execution of
1145 smooth pursuit. *Vision Res* 48: 2062-2069, 2008.
1146 **Jeffery KJ**. Learning of landmark stability and instability by hippocampal place cells.
1147 *Neuropharmacology* 37: 677-687, 1998.
1148 **Keele SW and Posner MI**. Processing of visual feedback in rapid movements. *Journal of*
1149 *Experimental Psychology* 77: 155-158, 1968.
1150 **Khan AZ, Pisella L, Rossetti Y, Vighetto A, and Crawford JD**. Impairment of gaze-centered
1151 updating of reach targets in bilateral parietal-occipital damaged patients. *Cereb Cortex* 15: 1547-
1152 1560, 2005a.
1153 **Khan AZ, Pisella L, Vighetto A, Cotton F, Luaute J, Boisson D, Salemme R, Crawford JD,**
1154 **and Rossetti Y**. Optic ataxia errors depend on remapped, not viewed, target location. *Nat*
1155 *Neurosci* 8: 418-420, 2005b.
1156 **Knill DC**. Learning Bayesian priors for depth perception. *J Vis* 7: 13, 2007a.
1157 **Knill DC**. Reaching for visual cues to depth: the brain combines depth cues differently for motor
1158 control and perception. *J Vis* 5: 103-115, 2005.
1159 **Knill DC**. Robust cue integration: a Bayesian model and evidence from cue-conflict studies with
1160 stereoscopic and figure cues to slant. *J Vis* 7: 5 1-24, 2007b.
1161 **Knill DC and Saunders JA**. Do humans optimally integrate stereo and texture information for
1162 judgments of surface slant? *Vision Res* 43: 2539-2558, 2003.
1163 **Koch G, Oliveri M, Torriero S, Carlesimo GA, Turriziani P, and Caltagirone C**. rTMS
1164 evidence of different delay and decision processes in a fronto-parietal neuronal network activated
1165 during spatial working memory. *Neuroimage* 24: 34-39, 2005.
1166 **Kording KP, Beierholm U, Ma WJ, Quartz S, Tenenbaum JB, and Shams L**. Causal
1167 inference in multisensory perception. *PLoS One* 2: e943, 2007.
1168 **Kording KP and Wolpert DM**. Bayesian integration in sensorimotor learning. *Nature* 427: 244-
1169 247, 2004.
1170 **Krigolson O, Clark N, Heath M, and Binsted G**. The proximity of visual landmarks impacts
1171 reaching performance. *Spat Vis* 20: 317-336, 2007.
1172 **Krigolson O and Heath M**. Background visual cues and memory-guided reaching. *Hum Mov*
1173 *Sci* 23: 861-877, 2004.
1174 **Lemay M, Bertram CP, and Stelmach GE**. Pointing to an allocentric and egocentric
1175 remembered target. *Motor Control* 8: 16-32, 2004.
1176 **McGuire LM and Sabes PN**. Sensory transformations and the use of multiple reference frames
1177 for reach planning. *Nat Neurosci* 12: 1056-1061, 2009.
1178 **Medendorp WP and Crawford JD**. Visuospatial updating of reaching targets in near and far
1179 space. *Neuroreport* 13: 633-636, 2002.
1180 **Medendorp WP, Goltz HC, Vilis T, and Crawford JD**. Gaze-centered updating of visual
1181 space in human parietal cortex. *J Neurosci* 23: 6209-6214, 2003a.
1182 **Medendorp WP, Tweed DB, and Crawford JD**. Motion parallax is computed in the updating
1183 of human spatial memory. *J Neurosci* 23: 8135-8142, 2003b.
1184 **Merriam EP, Genovese CR, and Colby CL**. Remapping in human visual cortex. *J*
1185 *Neurophysiol* 97: 1738-1755, 2007.

1186 **Merriam EP, Genovese CR, and Colby CL**. Spatial updating in human parietal cortex. *Neuron*
1187 39: 361-373, 2003.
1188 **Neely KA, Tessmer A, Binsted G, and Heath M**. Goal-directed reaching: movement strategies
1189 influence the weighting of allocentric and egocentric visual cues. *Exp Brain Res* 186: 375-384,
1190 2008.
1191 **Neggers SF, Scholvinck ML, van der Lubbe RH, and Postma A**. Quantifying the interactions
1192 between allo- and egocentric representations of space. *Acta Psychol (Amst)* 118: 25-45, 2005.
1193 **Niemeier M, Crawford JD, and Tweed DB**. Optimal transsaccadic integration explains
1194 distorted spatial perception. *Nature* 422: 76-80, 2003.
1195 **Obhi SS and Goodale MA**. The effects of landmarks on the performance of delayed and real-
1196 time pointing movements. *Exp Brain Res* 167: 335-344, 2005.
1197 **Olson CR and Gettner SN**. Object-centered direction selectivity in the macaque supplementary
1198 eye field. *Science* 269: 985-988, 1995.
1199 **Olson CR and Tremblay L**. Macaque supplementary eye field neurons encode object-centered
1200 locations relative to both continuous and discontinuous objects. *J Neurophysiol* 83: 2392-2411,
1201 2000.
1202 **Pasupathy A and Connor CE**. Population coding of shape in area V4. *Nat Neurosci* 5: 1332-
1203 1338, 2002.
1204 **Paulignan Y, MacKenzie C, Marteniuk R, and Jeannerod M**. Selective perturbation of visual
1205 input during prehension movements. 1. The effects of changing object position. *Exp Brain Res*
1206 83: 502-512, 1991.
1207 **Pelli DG**. The VideoToolbox software for visual psychophysics: transforming numbers into
1208 movies. *Spat Vis* 10: 437-442, 1997.
1209 **Prime SL, Niemeier M, and Crawford JD**. Transsaccadic integration of visual features in a
1210 line intersection task. *Exp Brain Res* 169: 532-548, 2006.
1211 **Prime SL, Tsotsos L, Keith GP, and Crawford JD**. Visual memory capacity in transsaccadic
1212 integration. *Exp Brain Res* 180: 609-628, 2007.
1213 **Prime SL, Vesia M, and Crawford JD**. Transcranial magnetic stimulation over posterior
1214 parietal cortex disrupts transsaccadic memory of multiple objects. *J Neurosci* 28: 6938-6949,
1215 2008.
1216 **Robinson DA**. The use of control systems analysis in the neurophysiology of eye movements.
1217 *Annu Rev Neurosci* 4: 463-503, 1981.
1218 **Sabes PN, Breznen B, and Andersen RA**. Parietal representation of object-based saccades. *J*
1219 *Neurophysiol* 88: 1815-1829, 2002.
1220 **Schenk T**. An allocentric rather than perceptual deficit in patient D.F. *Nat Neurosci* 9: 1369-
1221 1370, 2006.
1222 **Schlag J and Schlag-Rey M**. Does microstimulation evoke fixed-vector saccades by generating
1223 their vector or by specifying their goal? *Exp Brain Res* 68: 442-444, 1987.
1224 **Sereno AB and Maunsell JH**. Shape selectivity in primate lateral intraparietal cortex. *Nature*
1225 395: 500-503, 1998.
1226 **Sheth BR and Shimojo S**. Extrinsic cues suppress the encoding of intrinsic cues. *J Cogn*
1227 *Neurosci* 16: 339-350, 2004.
1228 **Smeets JB, van den Dobbelsteen JJ, de Grave DD, van Beers RJ, and Brenner E**. Sensory
1229 integration does not lead to sensory calibration. *Proc Natl Acad Sci U S A* 103: 18781-18786,
1230 2006.

Snyder LH, Grieve KL, Brotchie P, and Andersen RA. Separate body- and world-referenced representations of visual space in parietal cortex. *Nature* 394: 887-891, 1998.
Taylor JR. *An introduction to error analysis : the study of uncertainties in physical measurements*. Sausalito, Calif.: University Science Books, 1997.
Thaler L and Todd JT. The use of head/eye-centered, hand-centered and allocentric representations for visually guided hand movements and perceptual judgments. *Neuropsychologia* 47: 1227-1244, 2009.
Thier P and Andersen RA. Electrical microstimulation distinguishes distinct saccade-related areas in the posterior parietal cortex. *J Neurophysiol* 80: 1713-1735, 1998.
Thier P and Andersen RA. Electrical microstimulation suggests two different forms of representation of head-centered space in the intraparietal sulcus of rhesus monkeys. *Proc Natl Acad Sci U S A* 93: 4962-4967, 1996.
van Beers RJ, Sittig AC, and Gon JJ. Integration of proprioceptive and visual position-information: An experimentally supported model. *J Neurophysiol* 81: 1355-1364, 1999.
van der Kamp J, Savelsbergh G, and Smeets J. Multiple information sources in interceptive timing. *Human Movement Science* 16: 787-821, 1997.
Vann SD, Aggleton JP, and Maguire EA. What does the retrosplenial cortex do? *Nat Rev Neurosci* 10: 792-802, 2009.
Vaziri S, Diedrichsen J, and Shadmehr R. Why does the brain predict sensory consequences of oculomotor commands? Optimal integration of the predicted and the actual sensory feedback. *J Neurosci* 26: 4188-4197, 2006.
Verhagen L, Dijkerman HC, Grol MJ, and Toni I. Perceptuo-motor interactions during prehension movements. *J Neurosci* 28: 4726-4735, 2008.
Zaehle T, Jordan K, Wustenberg T, Baudewig J, Dechent P, and Mast FW. The neural basis of the egocentric and allocentric spatial frame of reference. *Brain Res* 1137: 92-103, 2007.
Zelaznik HZ, Hawkins B, and Kisselburgh L. Rapid visual feedback processing in single-aiming movements. *J Mot Behav* 15: 217-236, 1983.

FIGURE CAPTIONS

Figure 1: A) Cue-conflict experiment. Subjects were presented briefly with a to-be-remembered target (yellow) surrounded by four vibrating landmarks (blue). At the end of a memory delay following target and landmark offset the landmarks reappeared at a slightly shifted location. After the second landmark offset, subjects reached to touch the remembered target location. The fixation cross made two jumps during the memory delay in order to induce gaze-shifts of small or large amplitude. B) Egocentric-variability control experiment. Conventions are identical to the main experiment, but with no visual landmarks. C) Allocentric-variability control experiment. Conventions are identical to the main experiment, but the landmark shift is much larger and subjects were to reach based on new landmark-relative target location.

Figure 2: A) Cue-conflict experiment. B) Egocentric-variability control experiment. Same as cue-conflict task without landmarks. C) Allocentric-variability control experiment. Same as cue-conflict, but landmark shift was large and subjects were to reach based on new landmark-relative target location. Variable reaching error in all three experiments was assumed to arise partly from a common motor source with covariance, Σ^m. Within the egocentric and allocentric control experiments additional variability was assumed to come from representational sources with covariances given by Σ_e and Σ_a, respectively. Within the cue-conflict experiment additional variability was assumed to come from a combination of egocentric *and* allocentric representational sources that depends on the stability parameter, *p*. D) Assuming our MLE model is accurate, it provides a way to recover Σ_e, Σ_a, Σ^m and *p* from the observed variable error in all three experiments. Based on the resulting values for Σ_e, Σ_a, and *p* the model is able to predict egocentric-allocentric weighting in the cue-conflict experiment. Note that the mean weighting of

reaching responses in the various cue-conflict experimental conditions constitutes a data set that has no *a priori* relationship with reaching variability.

Figure 3: A) Transformation procedure. After correcting all reaching endpoints for systematic reaching bias (see Methods) each response (small red circle) was transformed by translating, rotating, and scaling its position vector so that the original target (solid orange disc) would be at the origin of the new coordinate system and the allocentric location (large, dashed blue circle) would be at the (1,0) location. B) Overall effect of landmark according to shift direction. The orange disc at the center of the circular plot represents original target location, while the blue outer circle represents the set of possible allocentric locations. The mean allocentric weight for a given direction is represented by the intersection point of the solid black curve with the dashed gray line segment corresponding to that direction. The solid curve itself is a cubic spline interpolation of these intersection points and simply serves as a guide to the eye.

Figure 4: Target-relative reaching endpoints for one subject in the cue-conflict experiment divided according to the direction of landmark shift. For example, if on a given trial the landmarks shifted upwards and to the left relative to their initial position, then the target-relative reaching endpoint for that trial is plotted in the upper left panel as a filled black circle. The orange disc at the origin of each panel represents the target location on all trials, while the dashed blue arcs in each panel represent the possible *allocentric locations* (described in the text). The large empty red circle in each panel represents the means of the target-relative reaching data for that panel/shift direction.

Figure 5: Top two panels show sample small gaze shift and large gaze shift eye movement traces for one subject in the egocentric-variability control experiment. Subject gaze always starts at centre. Bottom left/right panel: All target-relative reaching endpoints generated by this subject in

the small/large gaze shift condition. Each filled circle represents one target-relative reaching endpoint, while the orange disc at the center of the panel represents the target location for all trials.

Figure 6: All target-relative reaching endpoints generated by this subject in all four conditions of the allocentric-variability control experiment. Each filled circle represents one target-relative reaching endpoint, while the orange disc at the center of the panel represents the target location for all trials. This subject shows a slight leftward reaching bias, but no such effect is seen across subjects.

Figur 7: Effect of experimental manipulations on allocentric weights. The orange disc at the center of each subplot represents target location, while the dashed blue circle represents the set of allocentric locations. Each dashed line segment corresponds to an angular bin, and its intersection with a solid, closed contour represents the mean allocentric weight for landmark shift directions in that bin averaged over subjects.

Figur 8: Top panel: Solid, blue bars are between-subjects means for direct-fit allocentric weights in the small and large landmark vibration conditions. Error bars are between-subjects S.E.M. Solid, red bars are predictions from our full reliability-dependent MLE model. Hollow bars are corresponding predictions from the reduced model, without the stability parameter. Bottom panel: Same as top, but with data grouped according to gaze shift amplitude. Statistical differences are at the $\alpha = 0.05$ level and are derived from Bootstrapping (see Appendix).

Supplementary Material

Supplementary Figure S1: Sample finger and eye movement traces for one subject in the cue-conflict experiment. Panels a, c, e and g each show vertical finger position and gaze direction from the end of the initial fixation period to the end of the reaching interval for one *sv_lgs, lv_sgs, sv_sgs,* and *lv_lgs* trial, respectively. The thinner curve starting at 0 deg represents gaze direction, while the thicker curve starting at 35 deg down represents the finger position as projected onto the plane containing the display screen. The empty rectangles represent the vertical locations and time periods during which the fixation cross was present (the initial fixation cross at 0 deg is omitted for clarity). The gray-filled solid rectangles represent the vertical location of the egocentric target while it was visible, while the gray-filled dashed rectangles represent the location that the target would have had if it had reappeared with the shifted landmarks (allocentric location). Panels b, d, f, and h show the same trials, but from the subjects perspective. Again, the thinner curve starting at 0 deg represents gaze direction, while the thicker curve entering from the lower right represents the finger position. Here, the filled circle represents the original target location, while the empty circle represents the allocentric location.

Supplementary Figure S2: Overall effect of landmark shift by subject. This Figure is identical to Figure 3B except that allocentric weight data is not averaged over subjects, but rather plotted separately for each subject (one circular plot per subject).

Supplementary Figure S3: Effect of experimental manipulations on direct-fit and MLE-predicted allocentric weights grouped by landmark shift direction. The orange disc at the center of each subplot represents target location, while the dashed blue circle represents the set of allocentric locations. Each dashed line segment corresponds to an angular bin of 90 degree width, and its

intersection with a solid, closed contour represents the mean allocentric weight for landmark shift directions in that bin averaged over subjects.

Supplementary Table S1. *Relationship between second presentation landmark-relative reaching endpoints and first presentation landmark-relative target location.*

Condition	Mean Correlation/Slope	Holm-Bonferroni p-value
	Cue-Conflict Experiment Correlation Coefficients	
Horizontal		
sv_sgs	*0.36±0.06*	*0.003*
sv_lgs	*0.35±0.05*	*0.001*
lv_sgs	*0.23±0.07*	*0.013*
lv_lgs	*0.35±0.06*	*0.004*
Vertical		
sv_sgs	*0.29±0.07*	*0.007*
sv_lgs	*0.26±0.07*	*0.008*
lv_sgs	*0.33±0.07*	*0.005*
lv_lgs	*0.28±0.06*	*0.005*
	Allocentric-Variability Control Experiment Correlation Coefficients	
Horizontal		
sv_sgs	*0.36±0.07*	*0.006*
sv_lgs	*0.40±0.07*	*0.006*
lv_sgs	*0.39±0.09*	*0.006*
lv_lgs	*0.45±0.05*	*0.0002*
Vertical		
sv_sgs	*0.43±0.05*	*0.0003*
sv_lgs	*0.47±0.08*	*0.002*
lv_sgs	*0.51±0.05*	*0.0002*
lv_lgs	*0.45±0.05*	*0.0002*
	Allocentric-Variability Control Experiment Slopes (comparison to one)	
Horizontal		
sv_sgs	*0.7±0.1*	*0.3*
sv_lgs	*0.8±0.1*	*1.0*
lv_sgs	*0.8±0.2*	*1.0*
lv_lgs	*0.86±0.09*	*1.0*
Vertical		
sv_sgs	*0.9±0.1*	*1.0*
sv_lgs	*1.0±0.2*	*1.0*
lv_sgs	*1.1±0.2*	*1.0*
lv_lgs	*1.0±0.1*	*1.0*

Values are between-subjects means +/- standard error of the mean.

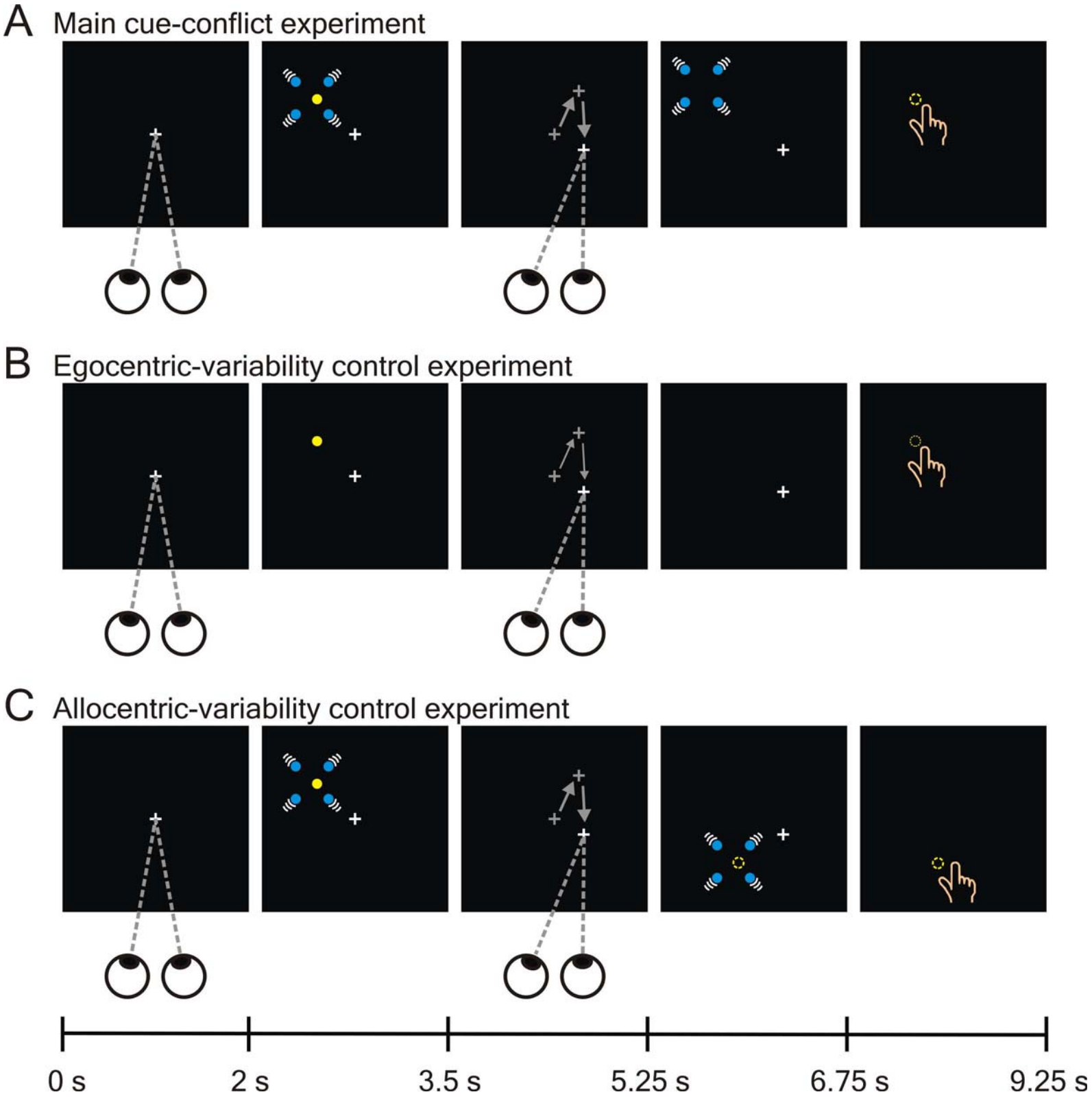
A
Main cue-conflict experiment
B
Egocentric-variability control experiment
C
Allocentric-variability control experiment
0 s
2 s
3.5 s
5.25 s
6.75 s
9.25 s

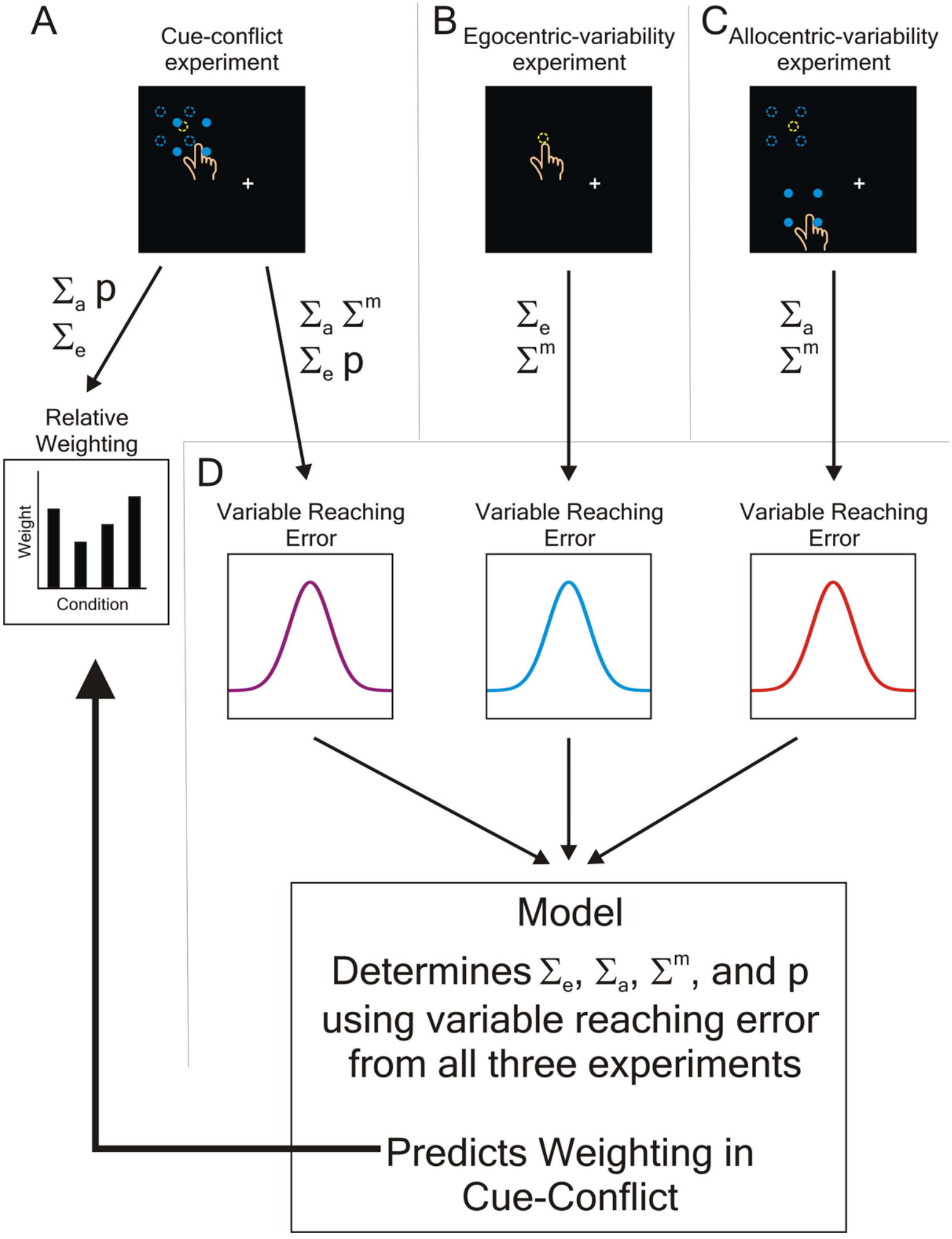
A
Cue-conflict experiment
B
Egocentric-variability experiment
C
Allocentric-variability experiment
Σ_a p
Σ_e
Σ_a Σ^m
Σ_e p
Σ_e
Σ^m
Σ_a
Σ^m
Relative Weighting
Weight
Condition
D
Variable Reaching Error
Variable Reaching Error
Variable Reaching Error
Model
Determines Σ_e, Σ_a, Σ^m, and p using variable reaching error from all three experiments
Predicts Weighting in Cue-Conflict

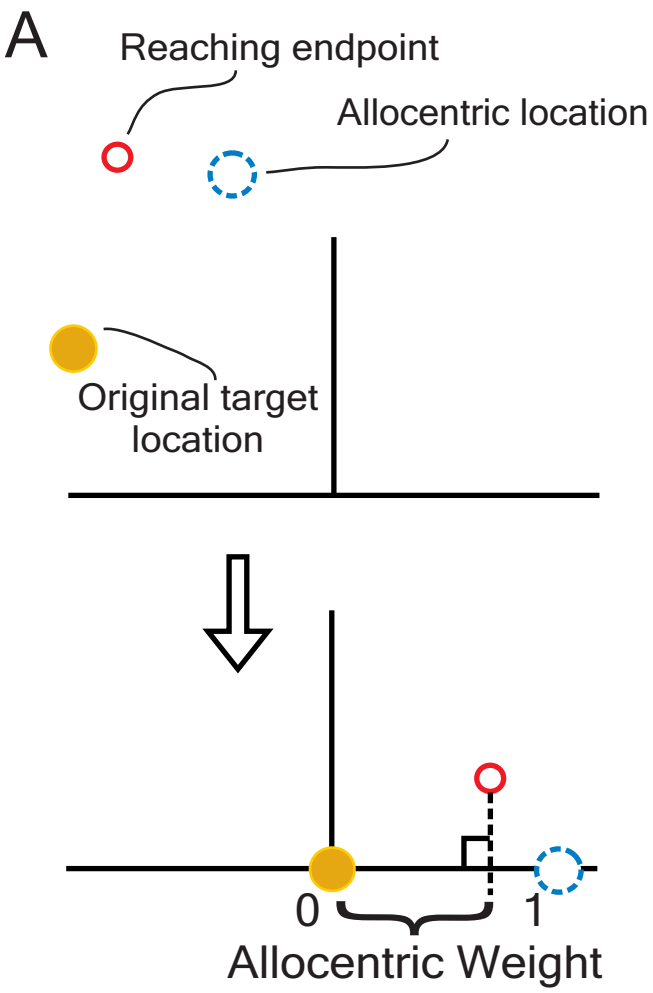
A
Reaching endpoint
Allocentric location
Original target location
0
1
Allocentric Weight

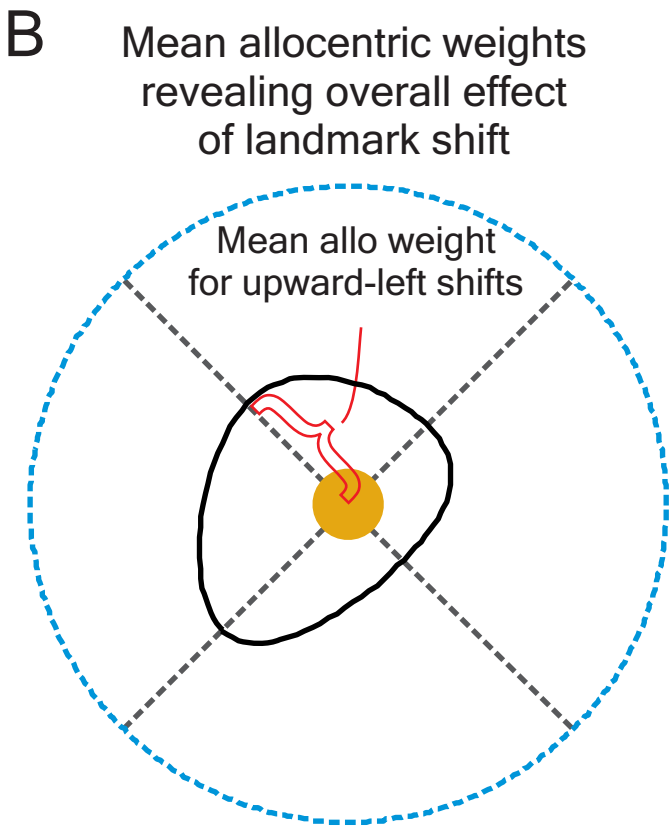
B
Mean allocentric weights revealing overall effect of landmark shift
Mean allo weight for upward-left shifts

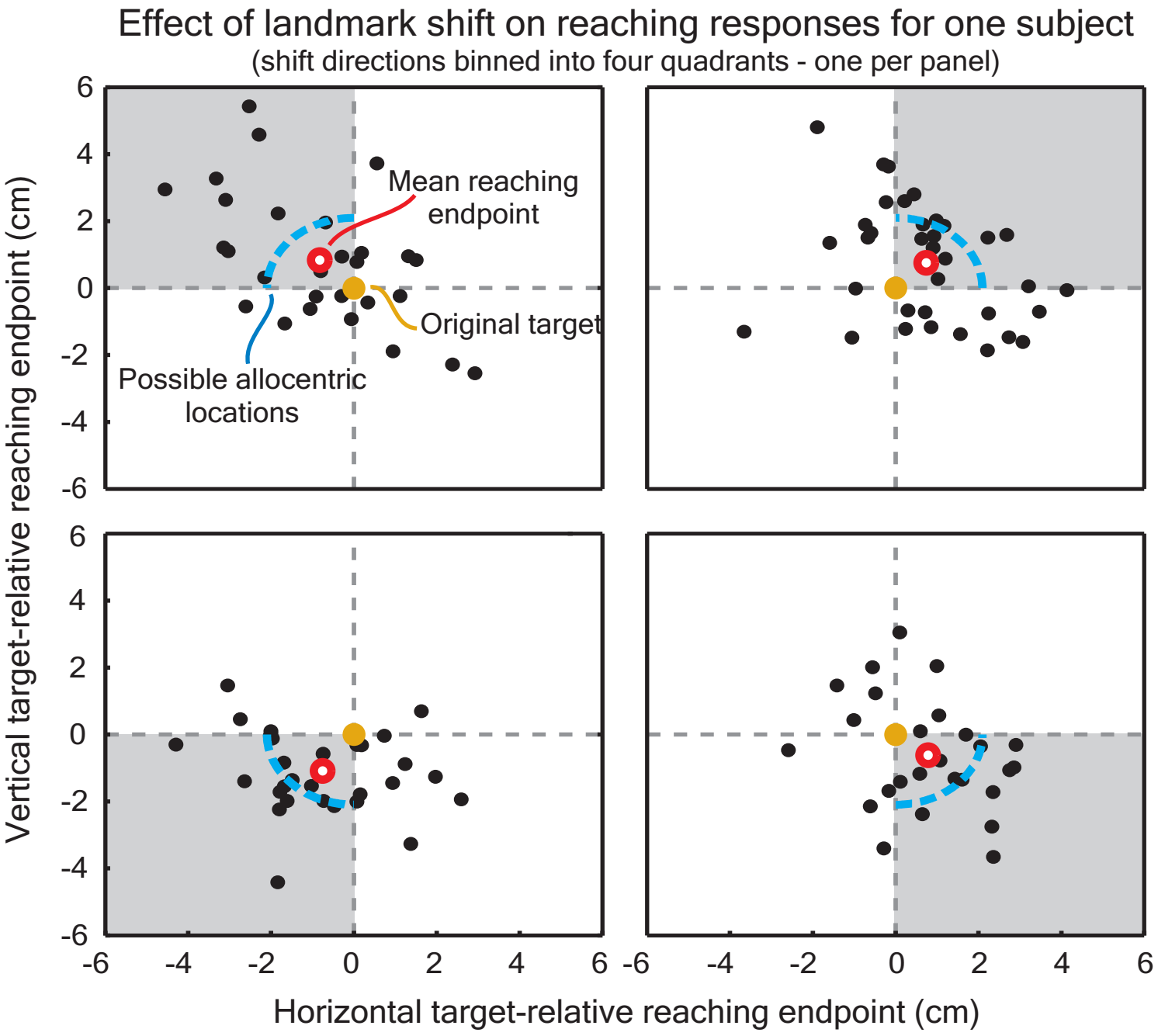
Effect of landmark shift on reaching responses for one subject
(shift directions binned into four quadrants - one per panel)
Mean reaching endpoint
Original target
Possible allocentric locations
Vertical target-relative reaching endpoint (cm)
Horizontal target-relative reaching endpoint (cm)
6
4
2
0
-2
-4
-6

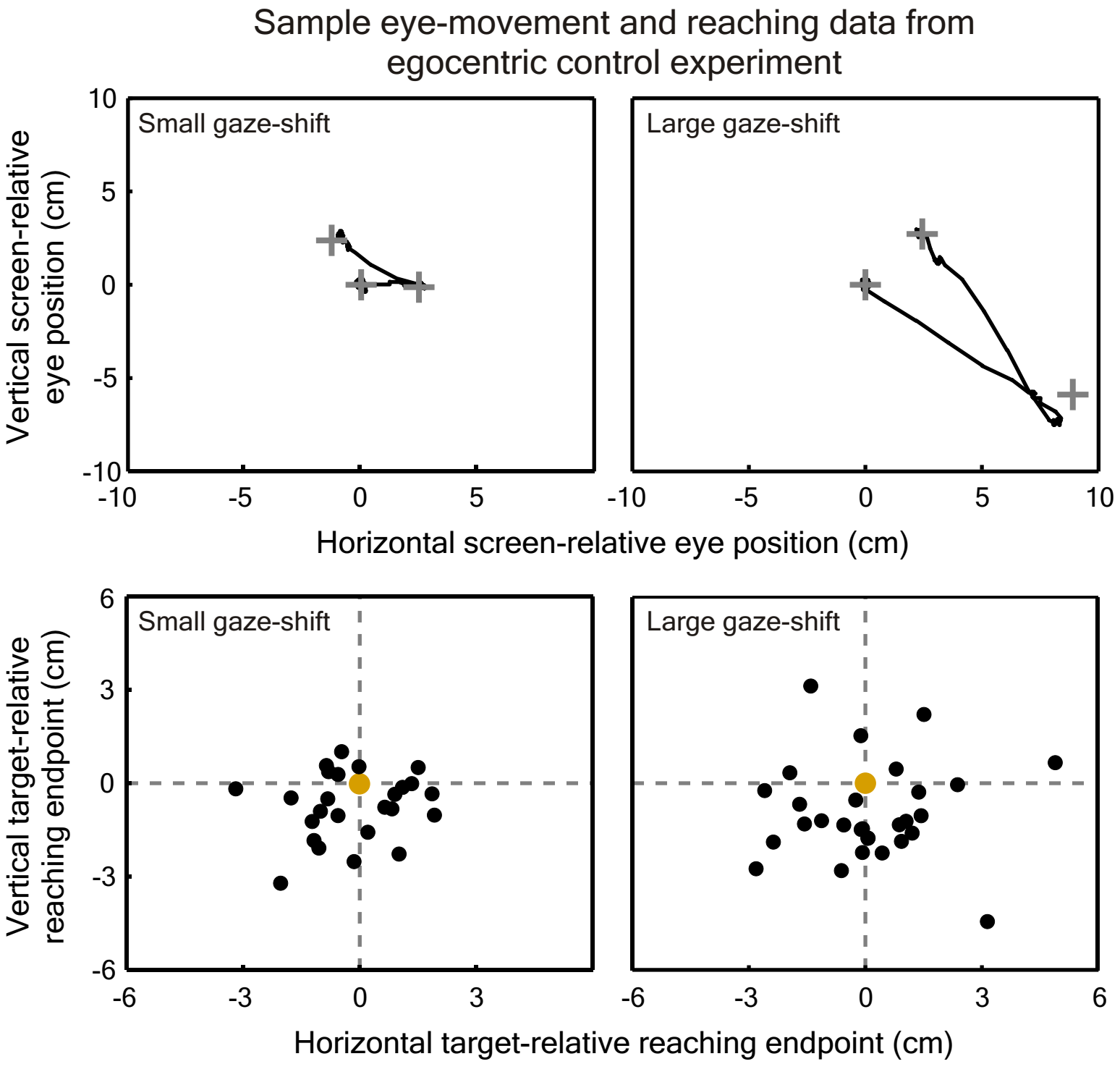
Sample eye-movement and reaching data from egocentric control experiment
Small gaze-shift
Large gaze-shift
Vertical screen-relative eye position (cm)
Horizontal screen-relative eye position (cm)
10
5
0
-5
-10
-10
-5
0
5
10
Small gaze-shift
Large gaze-shift
Vertical target-relative reaching endpoint (cm)
Horizontal target-relative reaching endpoint (cm)
6
3
0
-3
-6
-6
-3
0
3
6

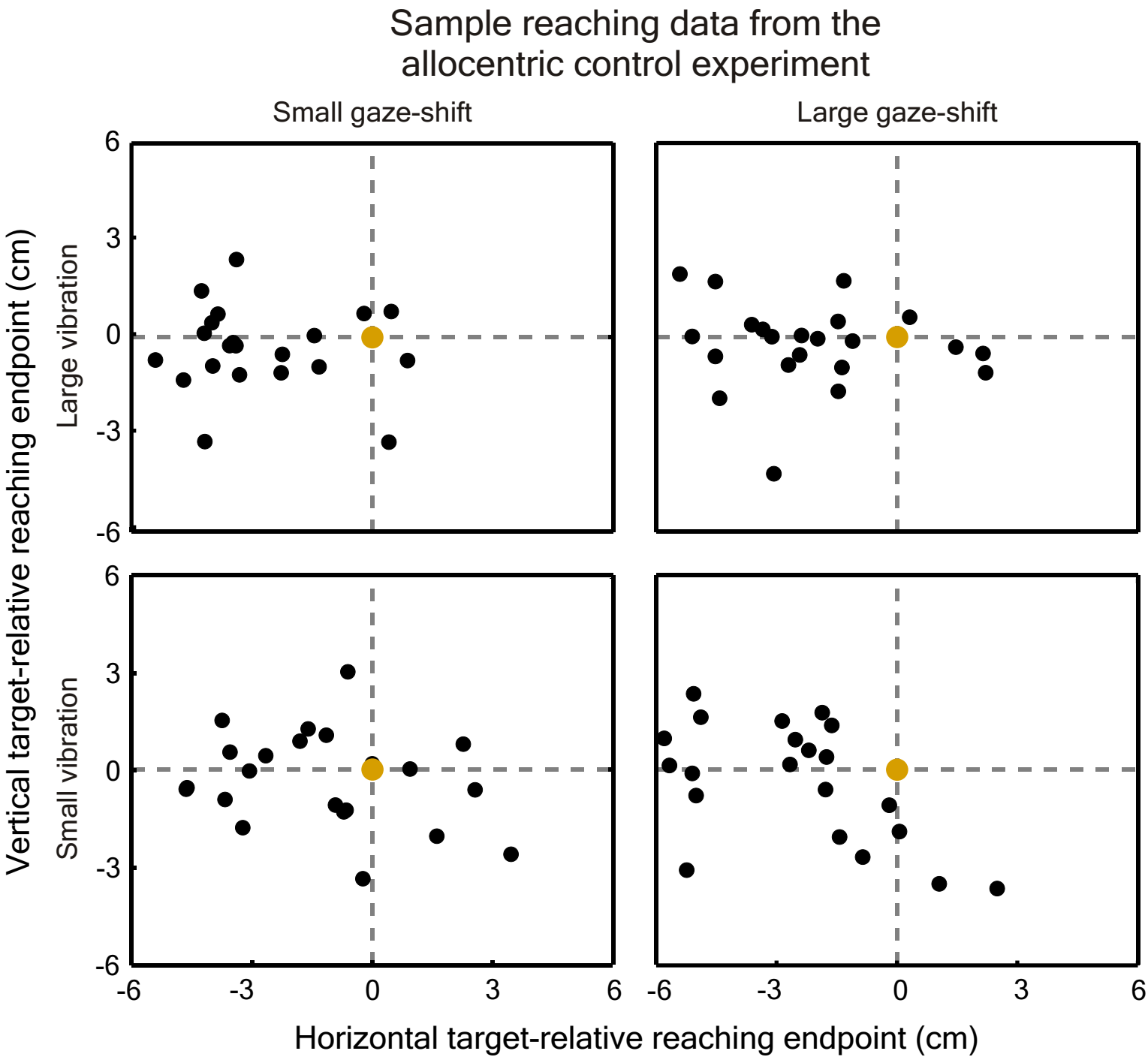
Sample reaching data from the
allocentric control experiment
Small gaze-shift
Large gaze-shift
Large vibration
Small vibration
Vertical target-relative reaching endpoint (cm)
Horizontal target-relative reaching endpoint (cm)
6
3
0
-3
-6
-6
-3
0
3
6

Allocentric weights grouped by landmark vibration amplitude

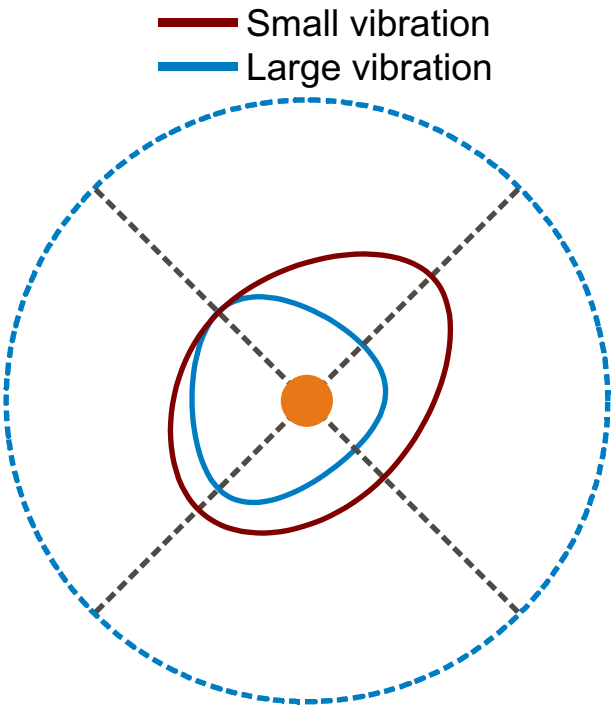

Allocentric weights grouped by gaze shift amplitude

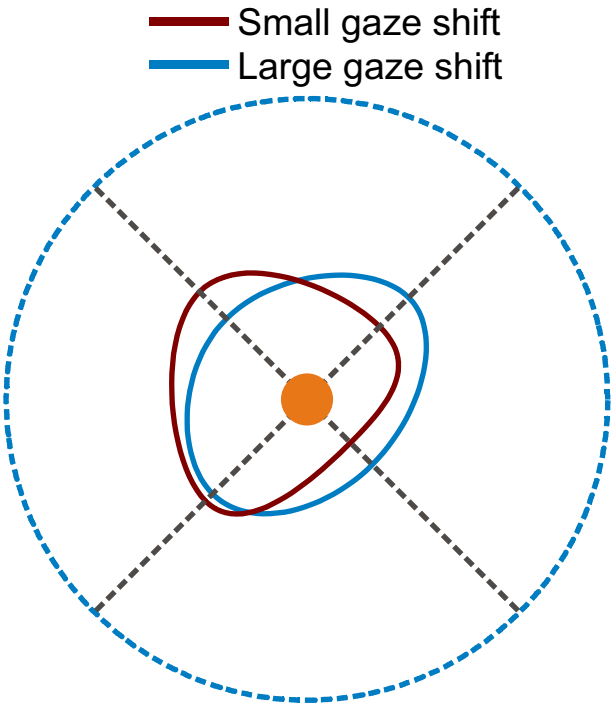

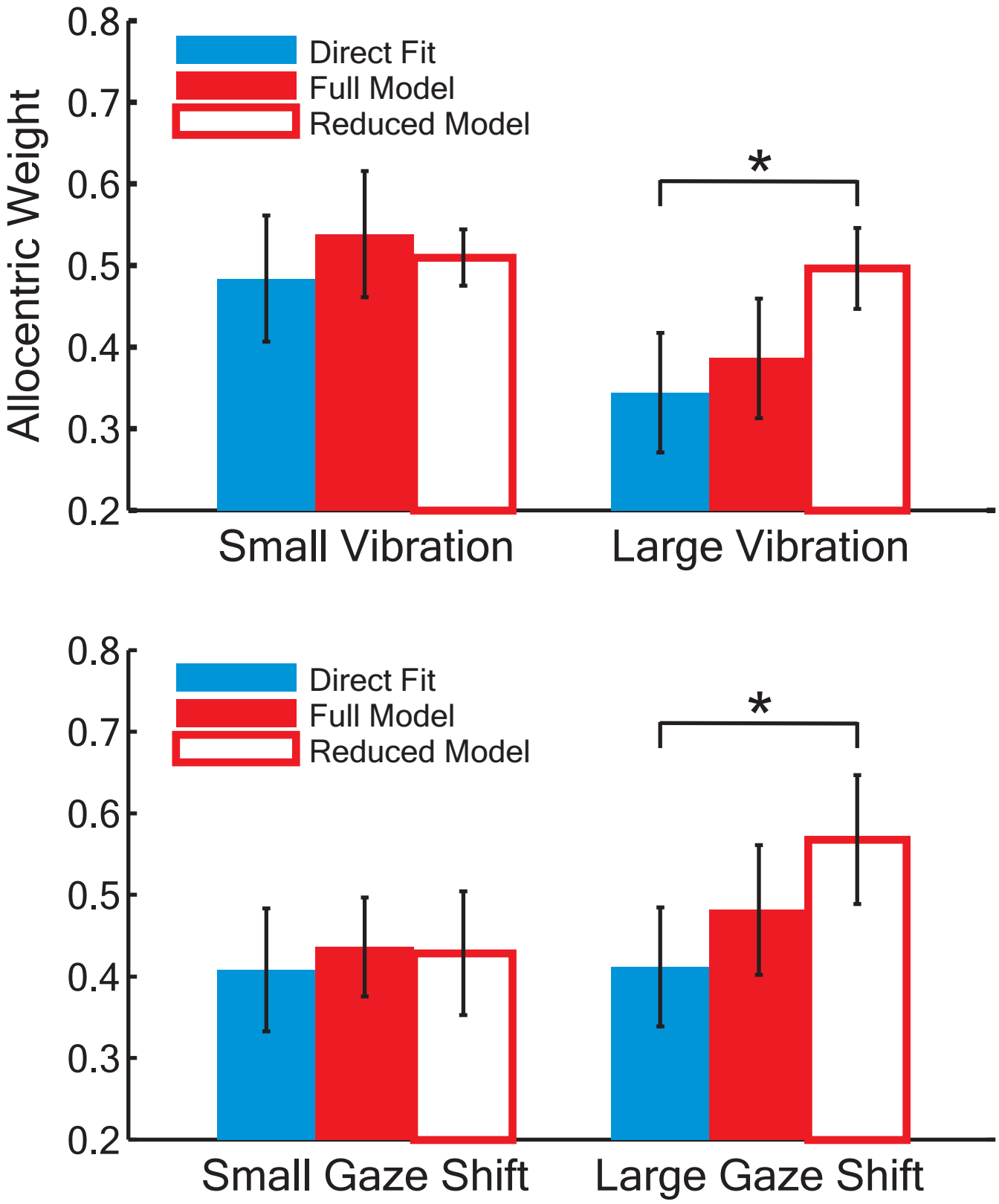
Allocentric Weight
0.8
0.7
0.6
0.5
0.4
0.3
0.2
Direct Fit
Full Model
Reduced Model
*
Small Vibration
Large Vibration
0.8
0.7
0.6
0.5
0.4
0.3
0.2
Direct Fit
Full Model
Reduced Model
*
Small Gaze Shift
Large Gaze Shift

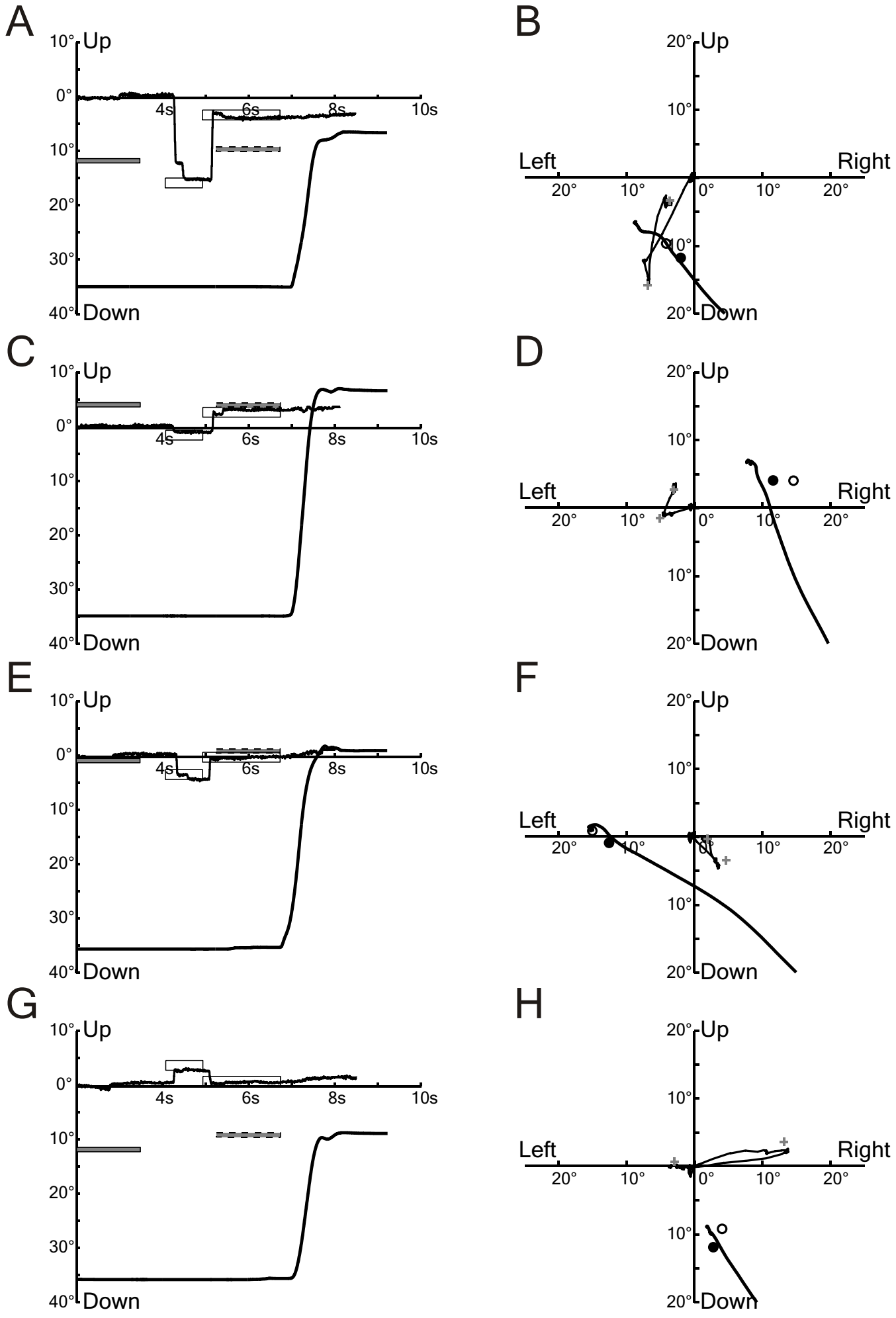
A
10° Up
0°
4s
6s
8s
10s
10°
20°
30°
40° Down
B
20° Up
10°
Left
Right
20°
10°
0°
10°
20°
10°
20° Down
C
10° Up
0°
4s
6s
8s
10s
10°
20°
30°
40° Down
D
20° Up
10°
Left
Right
20°
10°
0°
10°
20°
10°
20° Down
E
10° Up
0°
4s
6s
8s
10s
10°
20°
30°
40° Down
F
20° Up
10°
Left
Right
20°
10°
0°
10°
20°
10°
20° Down
G
10° Up
0°
4s
6s
8s
10s
10°
20°
30°
40° Down
H
20° Up
10°
Left
Right
20°
10°
0°
10°
20°
10°
20° Down

Weights for each subject revealing variability of shift effect

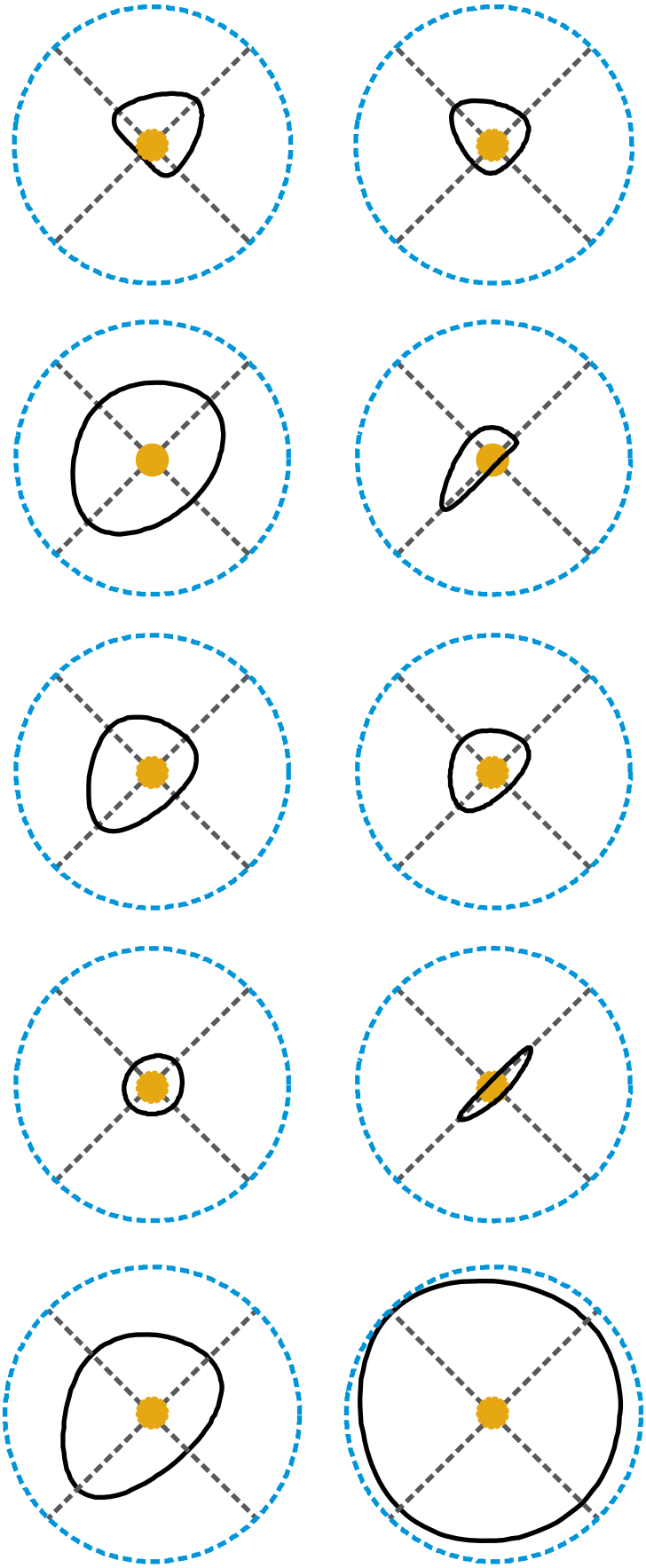

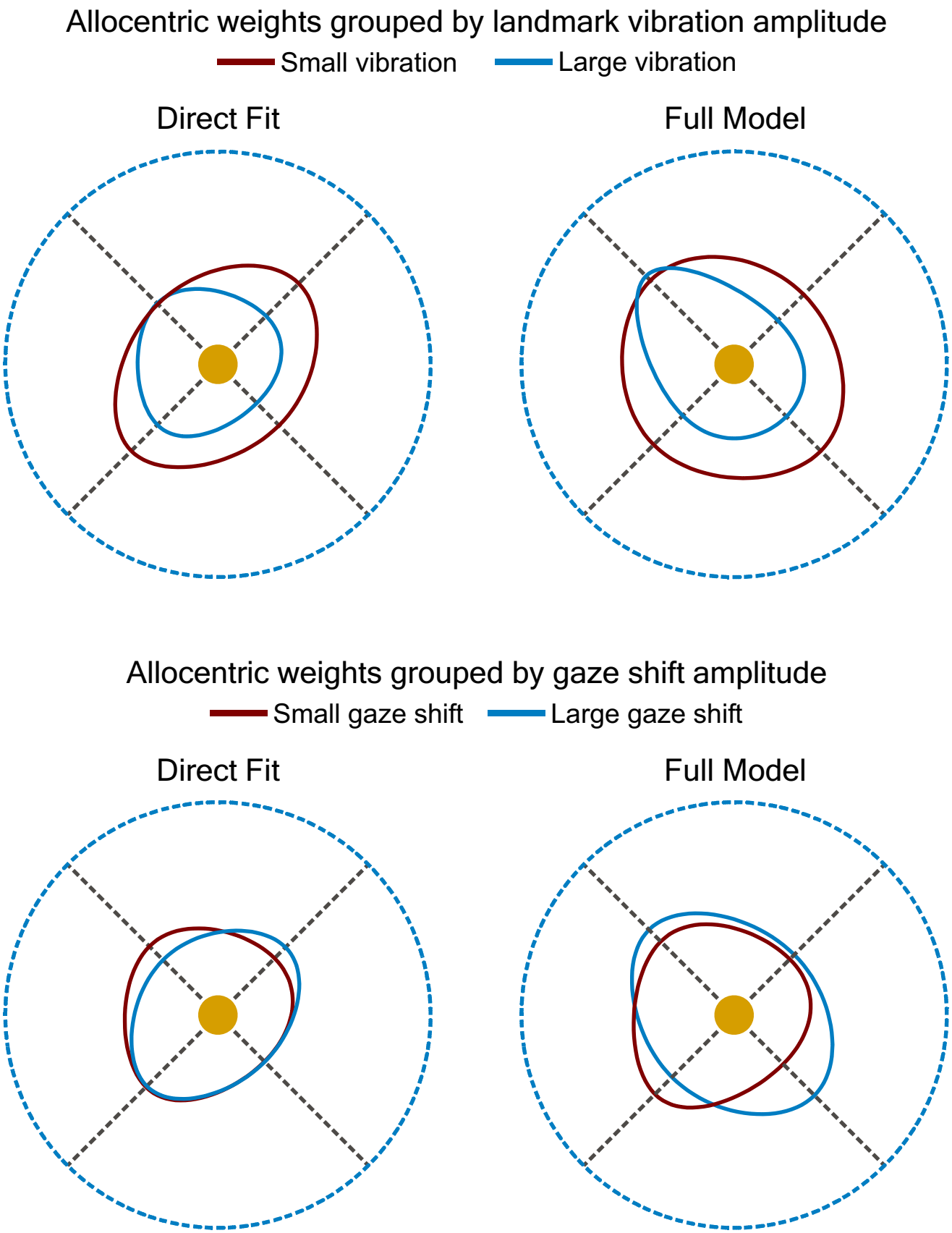
Allocentric weights grouped by landmark vibration amplitude
Small vibration
Large vibration
Direct Fit
Full Model
Allocentric weights grouped by gaze shift amplitude
Small gaze shift
Large gaze shift
Direct Fit
Full Model